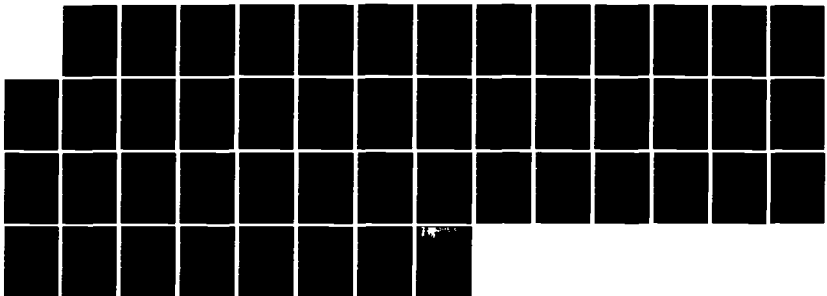


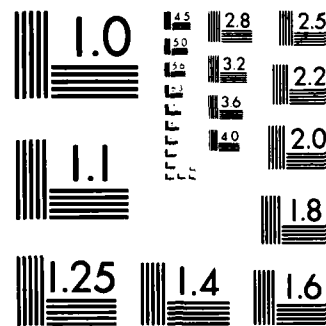
AD-A131 965 TECHNIQUE FOR PRODUCING A COHERENT SUM OF THE DATA FROM 1/1
P78-1 F2A AND F4 SATELLITES(U) EMMANUEL COLL BOSTON MA
E G HOLEMAN MAY 83 SCIENTIFIC-2 AFGL-TR-83-0130

UNCLASSIFIED F19628-82-K-0039

F/G 22/2

NL





MICROCOPY RESOLUTION TEST CHART
NATIONAL BUREAU OF STANDARDS 1963-A

(2)

AD A 131965

AFGL-TR-83-0130

Technique for Producing a Coherent Sum of the Data from P78-1,
F2, and F4 Satellites

Ernest G. Holeman

The Trustees of Emmanuel College
400 The Fenway
Boston MA 02115

May 1983

Scientific Report No. 2

DTIC

Approved for Public Release; distribution unlimited.

Air Force Geophysics Laboratory
Air Force Systems Command
United States Air Force
Hanscom AFB Massachusetts 01731

DTIC FILE COPY

83 08 25 070

Qualified requestors may obtain additional copies from the Defense Technical Information Center. All others should apply to the National Technical Information Service.

MIL-STD-847A
31 January 1973

Unclassified

SECURITY CLASSIFICATION OF THIS PAGE (When Data Entered)

REPORT DOCUMENTATION PAGE		READ INSTRUCTIONS BEFORE COMPLETING FORM						
1. REPORT NUMBER AFGL-TR-83-0130	2. GOVT ACCESSION NO. A.D.A. 31-1765	3. RECIPIENT'S CATALOG NUMBER						
4. TITLE (and Subtitle) Technique for Producing a Coherent Sum of the Data from P78-1, F2, and F4 Satellites		5. TYPE OF REPORT & PERIOD COVERED Scientific Report No. 2 01 Apr 82 - 31 Mar 83						
7. AUTHOR(s) Ernest G. Holeman		8. CONTRACT OR GRANT NUMBER(S) F19628-82-K-0039						
9. PERFORMING ORGANIZATION NAME AND ADDRESS Emmanuel College 400 The Fenway Boston MA 02115		10. PROGRAM ELEMENT, PROJECT, TASK AREA & WORK UNIT NUMBERS 62101F 760112AN						
11. CONTROLLING OFFICE NAME AND ADDRESS Air Force Geophysics Laboratory Hanscom AFB MA 01731 Contract Monitor: Irving Michael, PHC		12. REPORT DATE May 1983						
14. MONITORING AGENCY NAME & ADDRESS(if different from Controlling Office)		13. NUMBER OF PAGES 46						
		15. SECURITY CLASS. (of this report) Unclassified						
		16. DECLASSIFICATION/DOWNGRADING SCHEDULE						
16. DISTRIBUTION STATEMENT (of this Report) A - Approved for public release; distribution unlimited								
17. DISTRIBUTION STATEMENT (of the abstract entered in Block 20, if different from Report) TECH, OTHER								
18. SUPPLEMENTARY NOTES								
19. KEY WORDS (Continue on reverse side if necessary and identify by block number) <table><tr><td>Statfile</td><td>Spectral response</td></tr><tr><td>Noise spikes</td><td>Contour plots</td></tr><tr><td>Trapped radiation</td><td>Background analysis</td></tr></table>			Statfile	Spectral response	Noise spikes	Contour plots	Trapped radiation	Background analysis
Statfile	Spectral response							
Noise spikes	Contour plots							
Trapped radiation	Background analysis							
20. ABSTRACT (Continue on reverse side if necessary and identify by block number) Vertically incident data from the P78-1 J sensor was made available during the first quarter of 1983. It was sorted into a grid and time frame compatible with the F2 and F4 statfile data. In order to produce a coherent sum of the data from the three satellites into a final statfile product a consensus solution to several problems was agreed to.								

DD FORM 1 JAN 73 1473 EDITION OF 1 NOV 69 IS OBSOLETE

Unclassified

SECURITY CLASSIFICATION OF THIS PAGE (When Data Entered)

STATFILE DATA BASE NORMALIZATION AND CORRECTION

I. Vertically incident data from the P78-1 J sensor was made available during the first quarter of 1983. It was sorted into a grid and time frame compatible with the F2 and F4 statfile data. In order to produce a coherent sum of the data from the three satellites into a final statfile product a consensus solution to several problems was agreed to.

a) Noise spikes: An estimated 90% of the noise spikes remaining in the F2/F4 statfile were of the single channel type. These were eliminated using a simple count rate interpolation algorithm. If for a given spectrum the count rate in channel K was more than three times the sum of counts in channels K+1 and K-1, N_K was replaced by $(N_{K+1} + N_{K-1})/2$. For the border channels between the high and low energy heads, the interpolation was done between channels 7 and 10 taking into account the channel 8 to channel 9 geometrical factor ratio appropriately. For channel one, K-1 was set to 2 and for channel 16, K+1 was set to 15 making the algorithm complete. The remaining noise spikes were deemed ignorable and will be edited out by hand as required by future analysis or publication level graphics.

b) Background problems: A trapped radiation filter optimized for the F2 J package data was used for all three satellites to eliminate trapped radiation contamination. This filter algorithm worked very well for the F2 data but not so well for F4 and P78 because of spectral response differences among the three instruments compounded by complete lack of real calibration data. There are regions in geomagnetic latitude-magnetic local time space where F2 shows average count rates of less than 0.2 over the first 10 energy channels while the closest regions for F4 show a range of 0.25 to 1.41 and P78 a range of 0.68 to 1.47 for the 10 channels. In order to look at the background problem in detail, the statfile data for each satellite was combined into 18 average spectra by adding together the data for the two lowest Kp activity groups and combining the sum into 3 local time groups and six latitude groups with boundaries at 0, 8, 16, 24 hours for magnetic local time and 50, 60, 65, 70, 75, 80 and 90° for magnetic latitude. These spectra were labeled 1a, 1b, 1c, ... 6c for reference. The F2

data suggests that background levels exist (count rate levels below .5) for channels 1 through 10 for spectra 1a, 1b and 1c and for 2b over channels 1 through 8. There is only a small local time variation observed by F2. F4 data shows a much stronger gradient from high counts in 1a to background levels in 1c while P78 shows higher count rates in 1b with background levels in 1a and 1c. All three satellites show a background correction would be insignificant over spectra 3a through 5c except for channel 1 in the F4 data.

At this point, there is no way of knowing whether the local time variations are real temporal variations, a breakdown in the trapped radiation filter, local time dependent spacecraft charging effects or just electronic clutter effects due to local time dependent temperature variations. The consensus solution was to ignore its origin and treat it all as background. To do so, we subtracted the F2 1a, 1b and 1c spectra from the corresponding F4 and P78 spectra and defined that to be the background correction. For latitudes below 70° , the local time variation was kept while for latitudes above 70° , the smallest correction was used for all local times (1c for F4 and 1a for P78). See Table I for details of the background computation.

c) Variations in spectral response: Since there is no reason to expect large variations in the shape of the real average spectrum at a specific latitude and local time under similar geomagnetic activity conditions, it should be possible to use the statfile data for at least a relative recalibration giving a more consistent sum over the three satellites for the final statfile. To do so, we generated spectra 1a to 6c for each satellite for a moderate activity period (we used Kp groups 4 and 5, corresponding to $3- \leq Kp \leq 4+$). We reduced this to six spectra for each satellite by averaging over magnetic local time (labeling them 1d through 6d). Tables II and III summarize the results and give the F4/F2 and F4/P78 average spectra ratios as a function of latitude for channels 6 through 16. Also shown are the observed channel 8 to channel 9 counting rate ratios for each satellite.

The results clearly show a systematic variation of the spectral shape differences as a function of latitudes. The N8/N9 ratio for F2 suggests there is still significant trapped radiation leaking through

the filter at latitudes below 70°. The P78 data in comparison to F2 and F4 suggests that space craft charging effects could be shielding the instrument from lower energy electrons in both the F2 and F4 data.

The 4d spectra was selected as the best spectra for generating recalibration normalization factors. The F4 spectrum was selected as the base spectrum and F2 and P78 data normalized to F4 using the tabulated F4/F2 and F4/P78 data. The P78 spectra is probably closer to the real average spectra but was not selected as a base because of much smaller statistics then F2 or F4. The F2 was not selected because of the N8/N9 ratio greater than 3.0 whereas the calibration data we do have says the proper ratio should be approximately 2.4. Table IV gives the 4d ratios for channels 1 to 5.

- II. The three data bases were added together producing a final version of the statfile. The background corrections and normalization factors discussed above were used and Table V gives an explicit listing of them from the data reduction program. Appendix A gives a complete set of contour plots for the five quantities average energy (AEGY), energy flux (EFLX), integral flux (IFLX), Hall conductivity (HCON) and Pederson conductivity (PCON).

Accession For	
NTIS GRAFI	<input checked="" type="checkbox"/>
DTIC TAB	<input type="checkbox"/>
Unpublished	<input type="checkbox"/>
Justification	
By _____	
Date _____	
Att: _____	
Approved by _____	
Dist _____	
A	



TABLE I
F4-P78 Background Analysis at Lat = 50.5 (50 \leq LAT \leq 60)

	1	2	3	4	5	6	7	8	9	10	11
(a)											
F2	.31	.29	.19	.31	.24	.27	.30	.32	.16	.20	.85
F4	4.28	2.20	1.46	1.12	1.09	.78	.84	.80	1.24	—	3.33
P78	.51	.43	.43	.49	.58	.67	.77	1.16	1.39	1.36	1.49
(b)											
F2	.25	.25	.22	.21	.23	.25	.29	.28	.15	.31	1.12
F4	2.33	2.04	.97	.60	.60	.63	.82	.62	1.48	—	4.43
P78	1.07	1.05	1.08	1.10	1.15	1.31	1.49	1.86	2.38	2.38	4.51
(c)											
F2	.21	.19	.17	.15	.15	.16	.16	.16	.11	.15	.38
F4	1.41	.93	.54	.40	.30	.25	.31	.33	.63	—	1.47
P78	.76	.74	.68	.71	.77	.80	.89	1.11	1.47	1.37	1.63
F4-F2											
(a)	3.97	1.91	1.27	.81	.85	.51	.54	.48	1.08	—	2.48
(b)	2.08	1.81	.75	.39	.37	.38	.53	.34	1.33	—	3.31
(c)	1.20	.74	.37	.25	.15	.09	.15	.17	.52	—	1.09
P78-F2											
(a)	.20	.14	.24	.18	.34	.40	.47	.84	1.23	1.16	.64
(b)	.82	.82	.86	.89	.92	1.06	1.20	1.58	2.23	2.07	3.39
(c)	.55	.55	.51	.56	.62	.64	.73	.95	1.36	1.22	1.25

TABLE II
F2 to F4 Normalization

		6	7	8	9	10	11	12	13	14	15	16	N8/N9
	F4	.98	1.21	1.59	1.00	1.51	2.03	2.02	2.63	4.26	6.06	12.85	1.598
(51.0°)	F2	.77	.89	.99	.34	.50	1.13	1.48	2.28	3.65	4.68	14.64	2.912
(1d)	F4/F2	1.273	1.360	1.606	2.941	3.020	1.796	1.365	1.154	1.167	1.295	0.878	
	F4	78.24	80.53	80.35	26.80	29.32	31.84	32.74	33.49	35.23	36.86	44.16	2.998
(60.5°)	F2	91.42	99.44	102.88	12.68	14.35	17.26	19.40	21.81	23.83	25.94	33.65	8.114
(2d)	F4/F2	.856	.816	.781	2.114	2.043	1.845	1.688	1.536	1.478	1.421	1.312	
	F4	195.76	217.65	224.69	89.56	95.91	102.50	100.39	95.67	92.59	89.22	89.74	2.509
(65.5°)	F2	230.58	247.25	247.29	73.32	81.55	88.94	89.98	88.40	85.36	81.83	87.11	3.374
(3d)	F4/F2	.849	.880	.909	1.221	1.176	1.152	1.116	1.082	1.085	1.090	1.030	
	F4	127.44	159.94	196.51	79.78	111.23	142.67	171.43	188.23	192.36	184.95	172.25	2.463
(70.5°)	F2	188.33	249.34	318.24	100.60	126.55	163.05	181.89	187.46	181.41	169.96	162.32	3.163
(4d)	F4/F2	.677	.641	.617	.793	.879	.875	.942	1.004	1.060	1.088	1.061	
	F4	32.27	58.18	99.20	40.17	81.07	121.98	179.82	232.71	250.04	243.85	216.15	2.470
(75.5°)	F2	48.48	92.17	150.88	48.75	73.80	122.58	158.16	179.56	178.16	162.38	146.80	3.096
(5d)	F4/F2	.666	.631	.657	.824	1.099	.995	1.137	1.296	1.403	1.502	1.472	
	F4	3.70	9.04	18.19	7.84	14.49	21.16	30.67	40.35	46.67	47.24	43.58	2.320
(81°)	F2	10.21	19.00	35.12	11.05	16.45	28.78	38.75	43.20	42.14	38.19	34.72	3.179
(6d)	F4/F2	.362	.476	.518	.710	.881	.735	.791	.934	1.103	1.237	1.255	

TABLE III
P78 to F4 Normalization

		6	7	8	9	10	11	12	13	14	15	16	N8/N9
(51.0°) (1d)	F4	.98	1.21	1.59	1.00	1.51	2.03	2.02	2.63	4.26	6.06	12.85	1.598
	P78	5.87	6.85	7.96	3.62	4.32	5.54	8.60	11.77	13.79	16.36	82.11	2.199
	F4/P78	.167	.177	.200	.276	.350	.366	.235	.223	.309	.370	.156	
(60.5°) (2d)	F4	78.24	80.53	80.35	26.80	29.32	31.84	32.74	33.49	35.23	36.86	44.16	2.998
	P78	124.88	128.60	132.62	53.89	57.30	62.30	60.90	65.63	68.49	74.44	155.19	2.461
	F4/P78	.627	.626	.606	.497	.512	.511	.538	.510	.514	.495	.285	
(65.5°) (3d)	F4	195.76	217.65	224.69	89.56	95.91	102.50	100.39	95.67	92.59	89.22	89.74	2.509
	P78	167.06	201.20	227.99	96.38	105.28	109.81	115.74	120.29	121.76	132.52	204.56	2.366
	F4/P78	1.172	1.082	.986	.929	.911	.933	.867	.795	.760	.673	.439	
(70.5°) (4d)	F4	127.44	159.94	196.51	79.78	111.23	142.67	171.43	188.23	192.36	184.95	172.25	2.403
	P78	94.57	131.62	176.40	75.66	112.80	176.61	254.53	305.94	319.42	328.17	382.29	2.331
	F4/P78	1.548	1.215	1.114	1.054	.986	.808	.674	.615	.602	.564	.451	
(75.5°) (5d)	F4	32.27	58.18	99.20	40.17	81.07	121.82	179.82	232.71	250.04	243.85	216.15	2.470
	P78	24.13	41.28	70.21	30.77	68.40	135.78	226.95	282.57	291.46	284.99	312.05	2.282
	F4/P78	1.337	1.409	1.413	1.305	1.185	.898	.792	.824	.858	.856	.693	
(81°) (6d)	F4	3.70	9.04	18.19	7.84	14.49	21.16	30.67	40.35	46.67	47.24	43.58	2.320
	P78	4.18	7.64	18.12	7.80	20.62	37.89	57.11	68.69	65.23	66.21	86.77	2.323
	F4/P78	.888	1.183	1.004	1.005	.703	.558	.537	.587	.712	.713	.502	

TABLE IV
F2 & P78 Normalization to F4 High Energy Channels

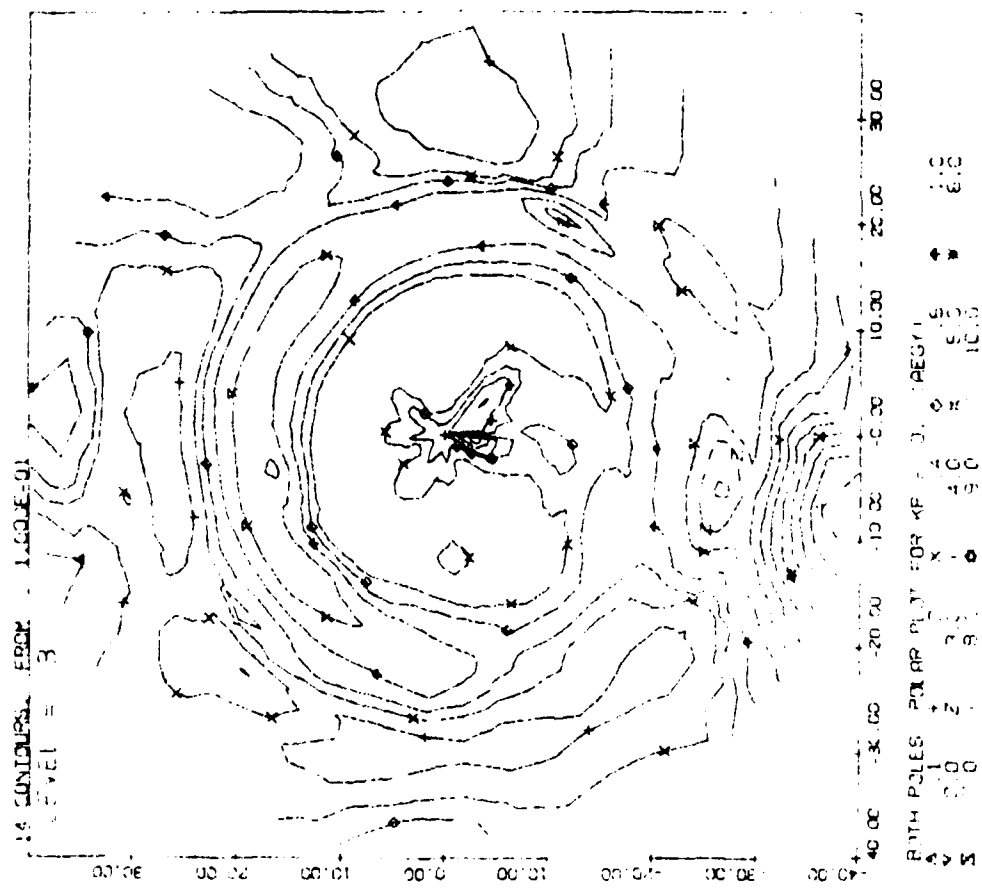
		1	2	3	4	5
(70.5°)	F4	6.18	14.49	32.65	61.58	92.99
(4d)	F2	10.15	20.36	50.24	87.93	137.01
	P78	5.35	10.96	21.48	41.11	69.76
	F4/F2	.608	.712	.650	.700	.679
	F4/P78	1.155	1.322	1.520	1.498	1.333

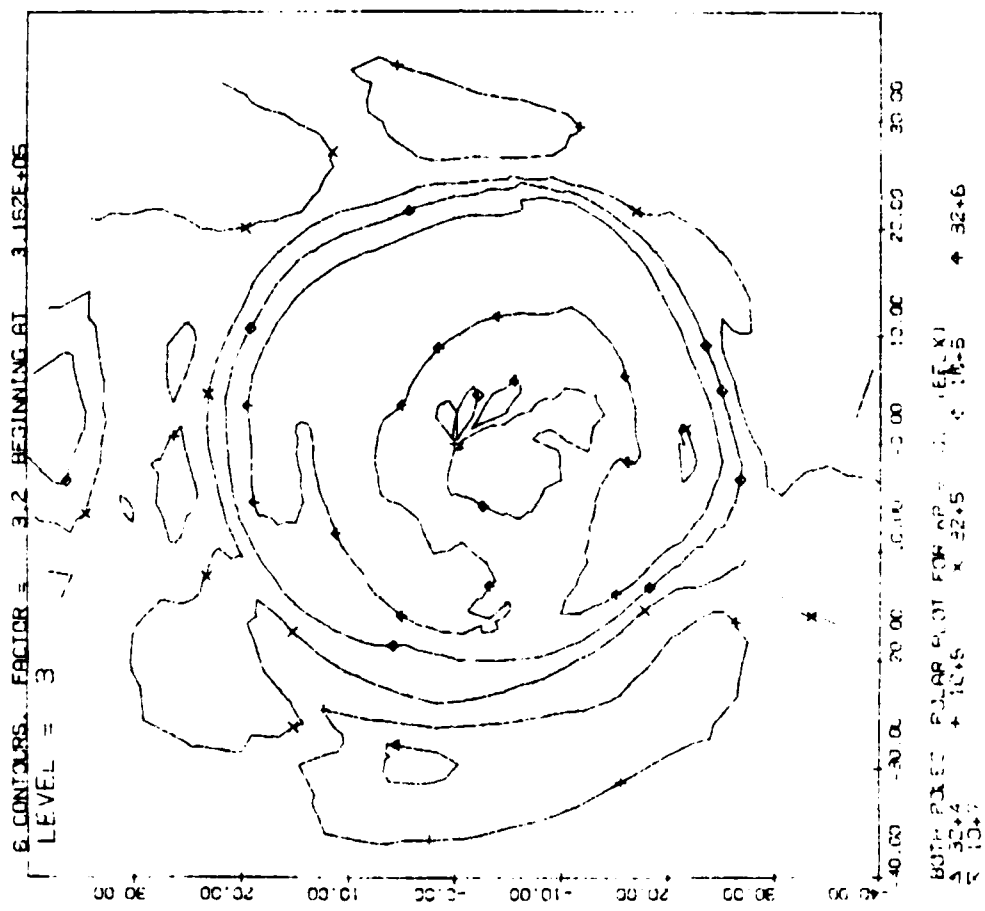
TABLE V
Summary of Corrections from Program

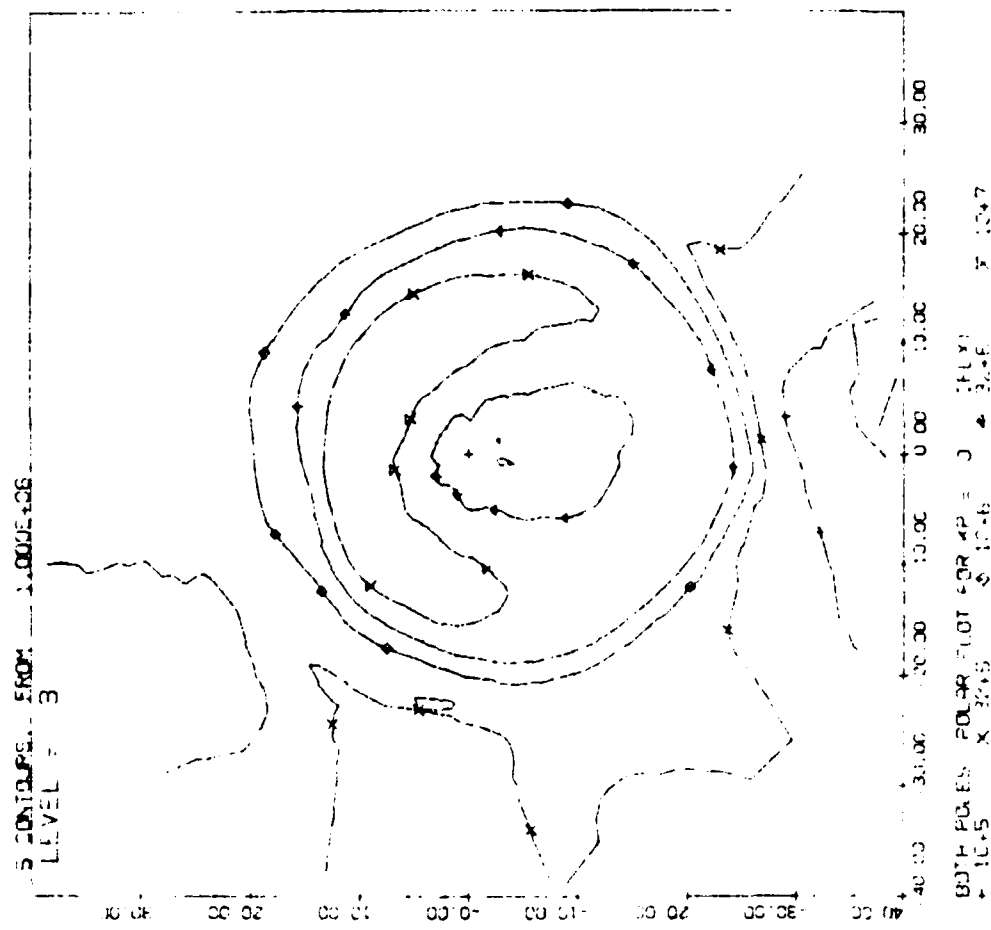
Ch#	Normalization				Background			
	F2NOP	P8DOR	F4	P78	F4	P78	F4	P78
			a	b	c	c		
1	.609	1.155	3.970	.200	2.080	.820	1.200	.550
2	.712	1.322	1.910	.140	1.810	.820	.740	.550
3	.650	1.520	1.270	.240	.750	.860	.370	.510
4	.700	1.498	.810	.180	.390	.890	.250	.560
5	.679	1.333	.850	.340	.370	.920	.150	.620
6	.677	1.348	.510	.400	.380	1.060	.090	.640
7	.641	1.215	.540	.470	.530	1.200	.150	.730
8	.617	1.114	.480	.840	.340	1.580	.170	.950
9	.793	1.054	1.080	1.230	1.330	2.230	.520	1.360
10	.879	.986	1.780	1.160	2.320	2.070	.810	1.220
11	.875	.808	2.480	.640	5.310	3.390	1.090	1.250
12	.942	.674	1.000	1.000	1.000	3.000	1.000	1.000
13	1.004	.615	1.000	1.000	1.000	3.000	1.000	1.000
14	1.060	.602	1.000	1.000	1.000	3.000	1.000	1.000
15	1.088	.564	1.000	1.000	1.000	3.000	1.000	1.000
16	1.061	.451	1.000	1.000	1.000	1.000	1.000	1.000

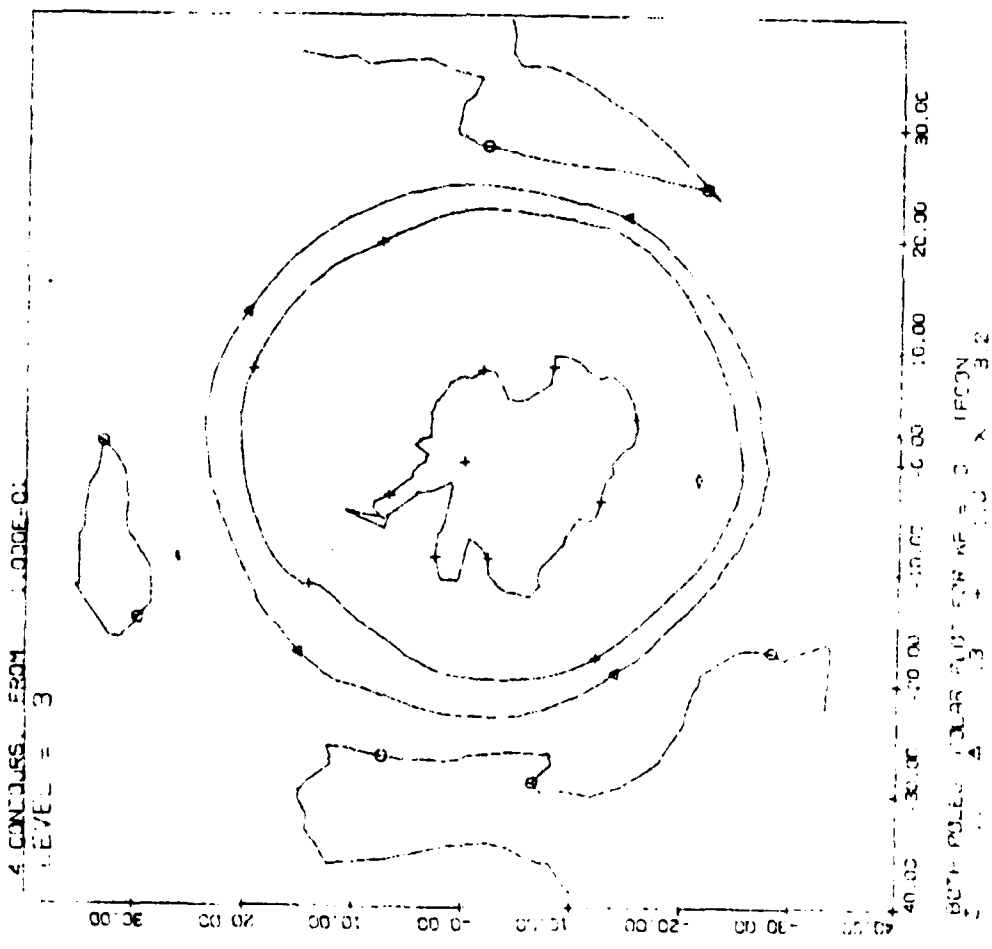
APPENDIX A

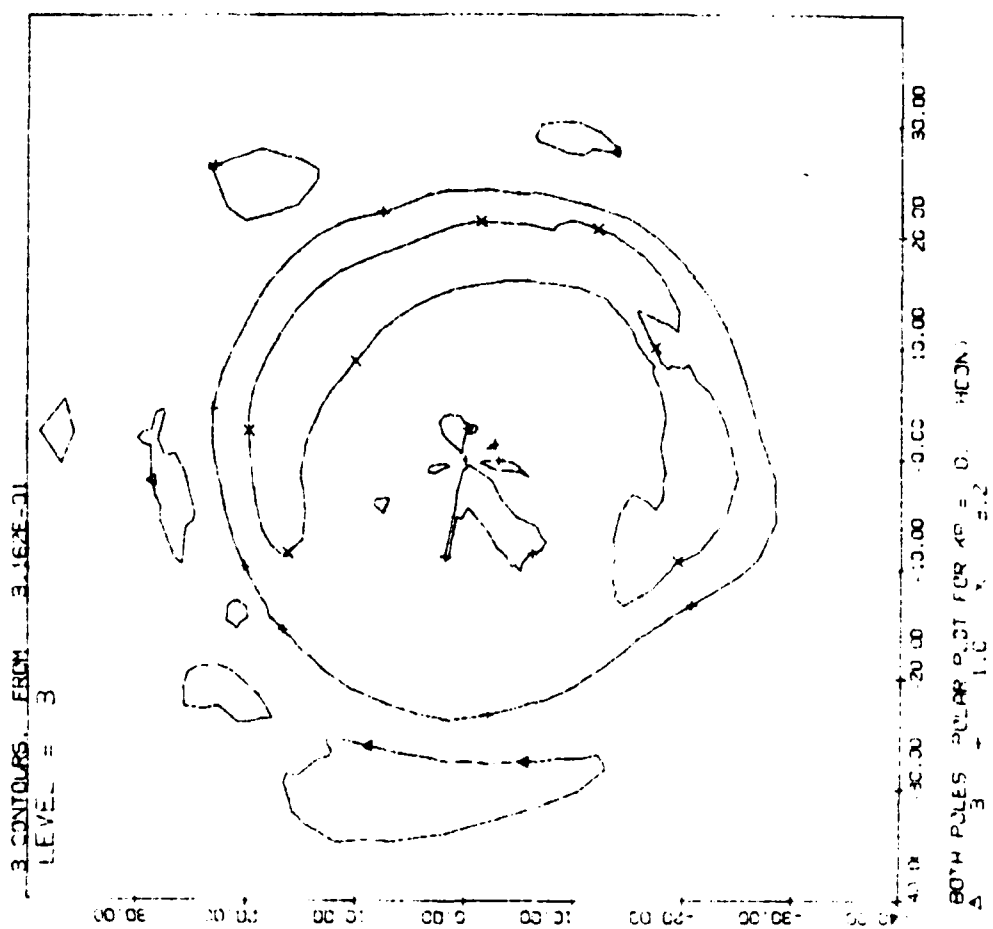
Contour Plots

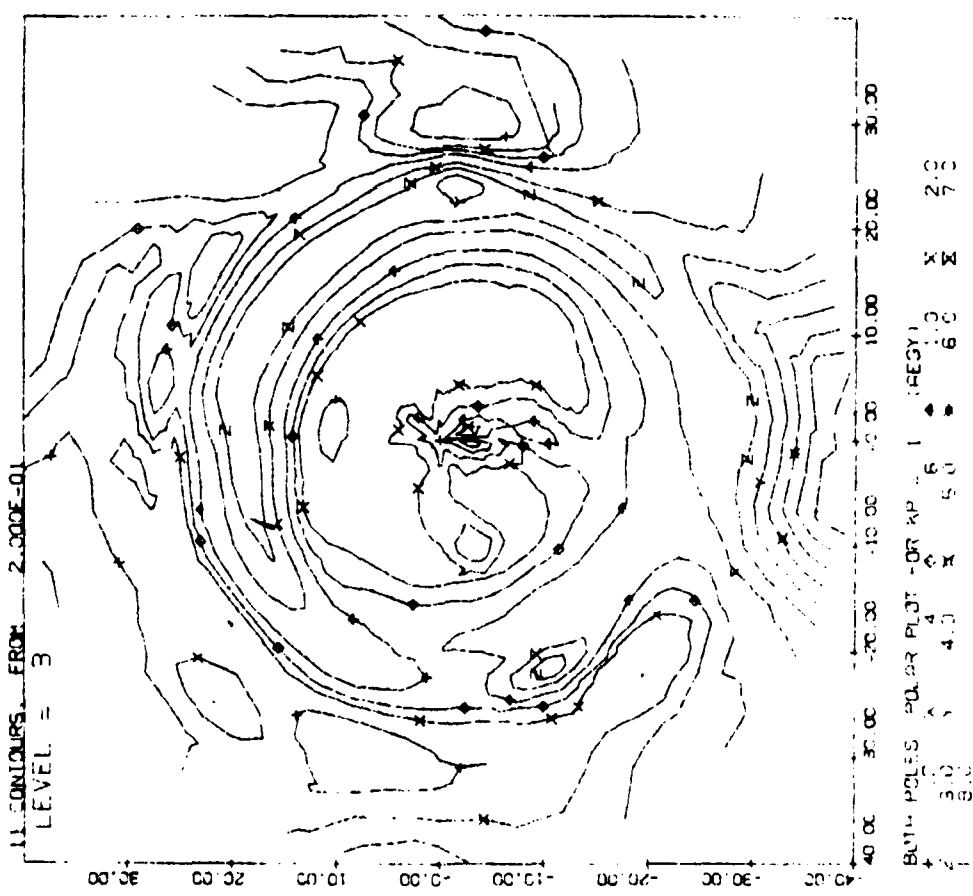


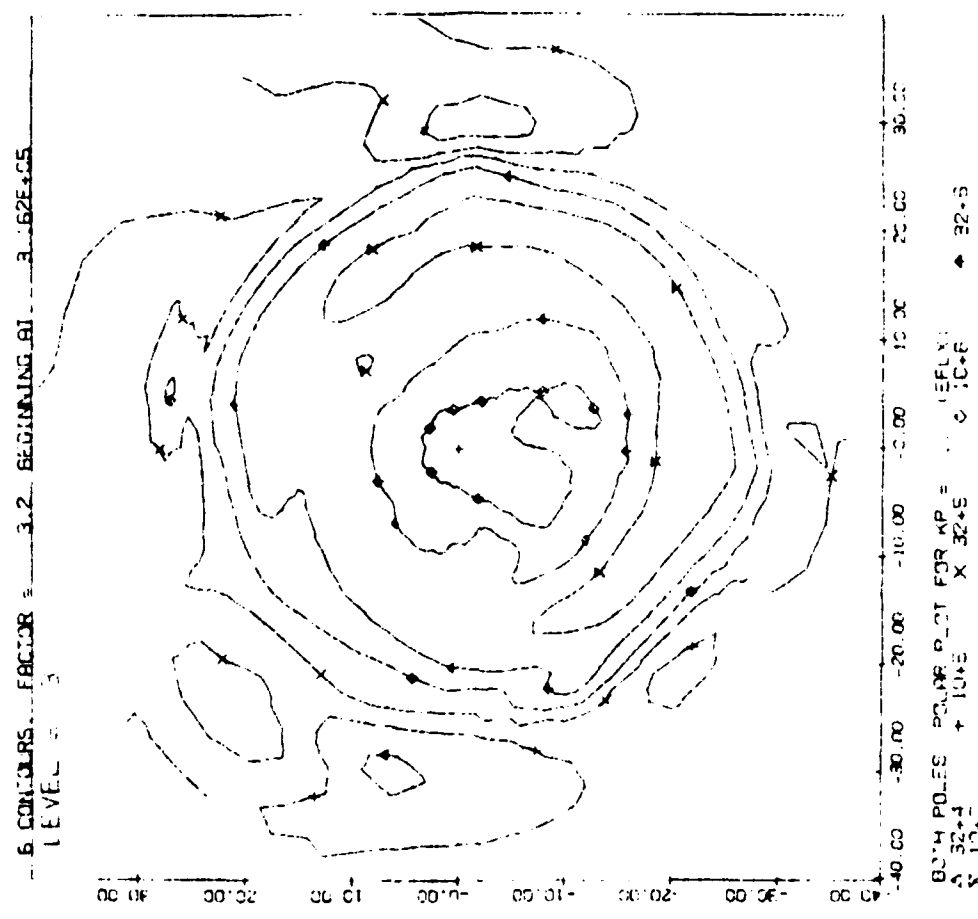


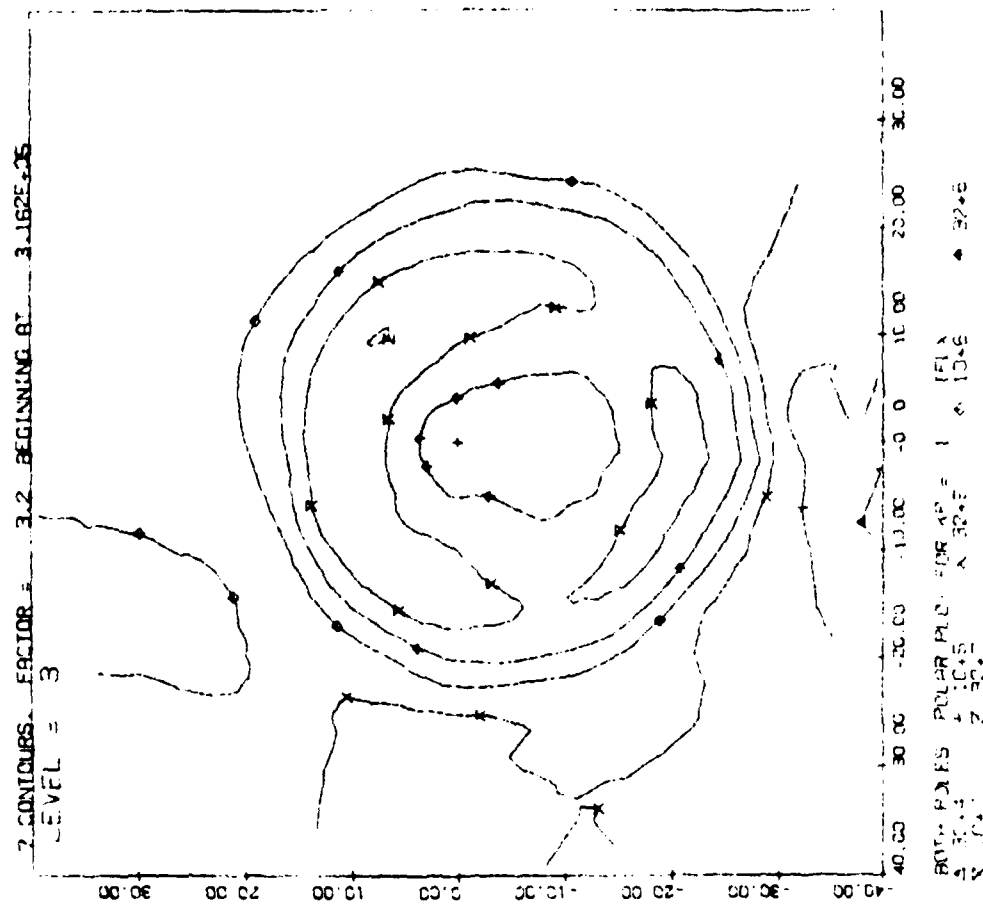


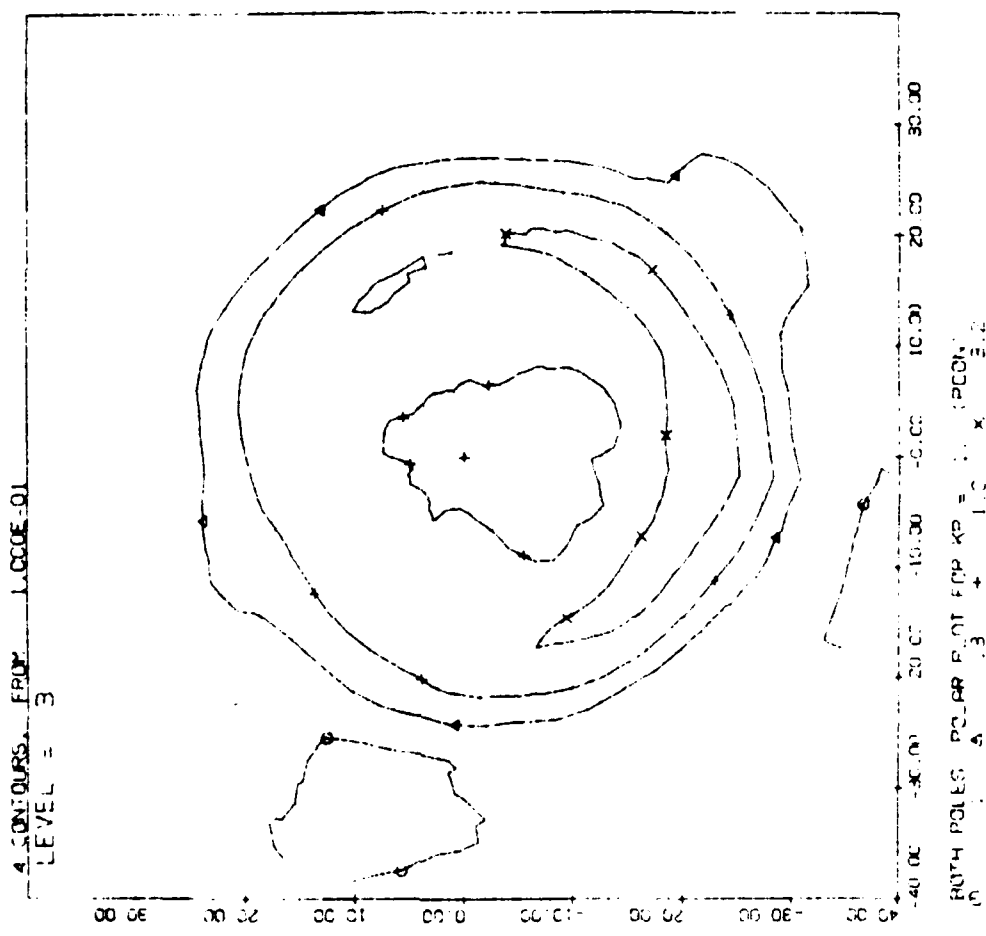


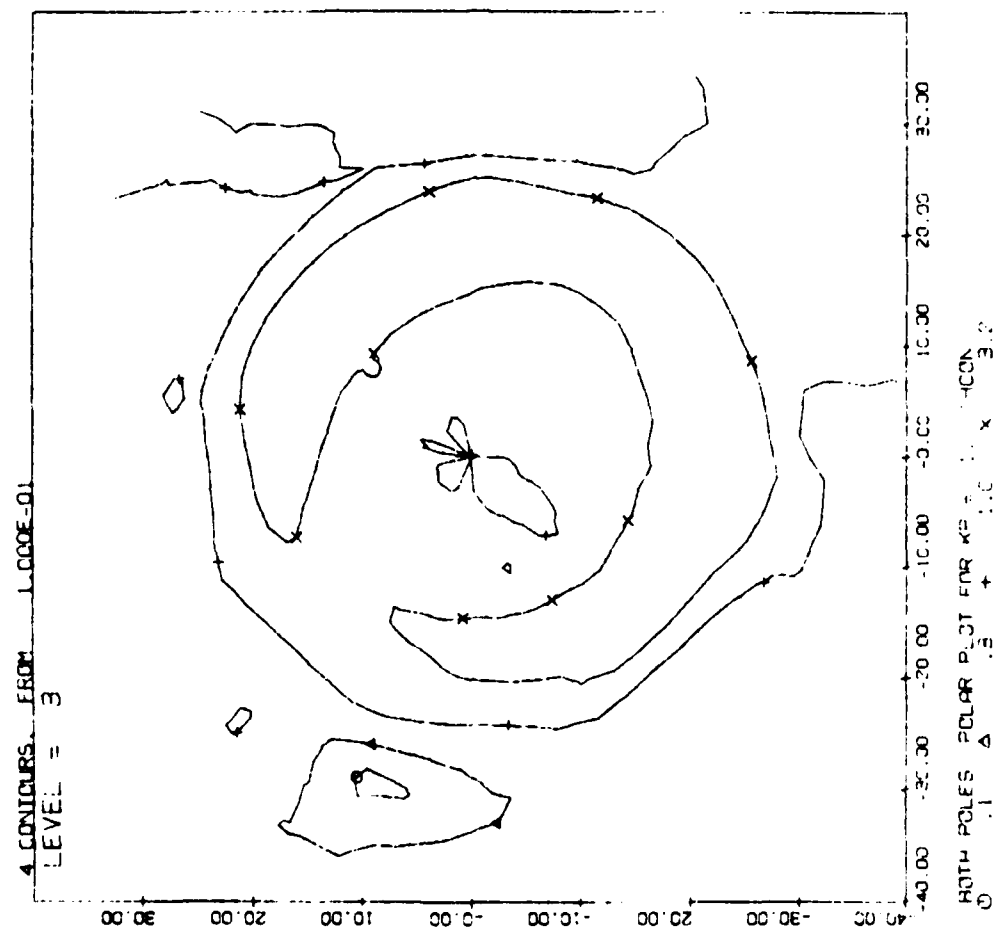


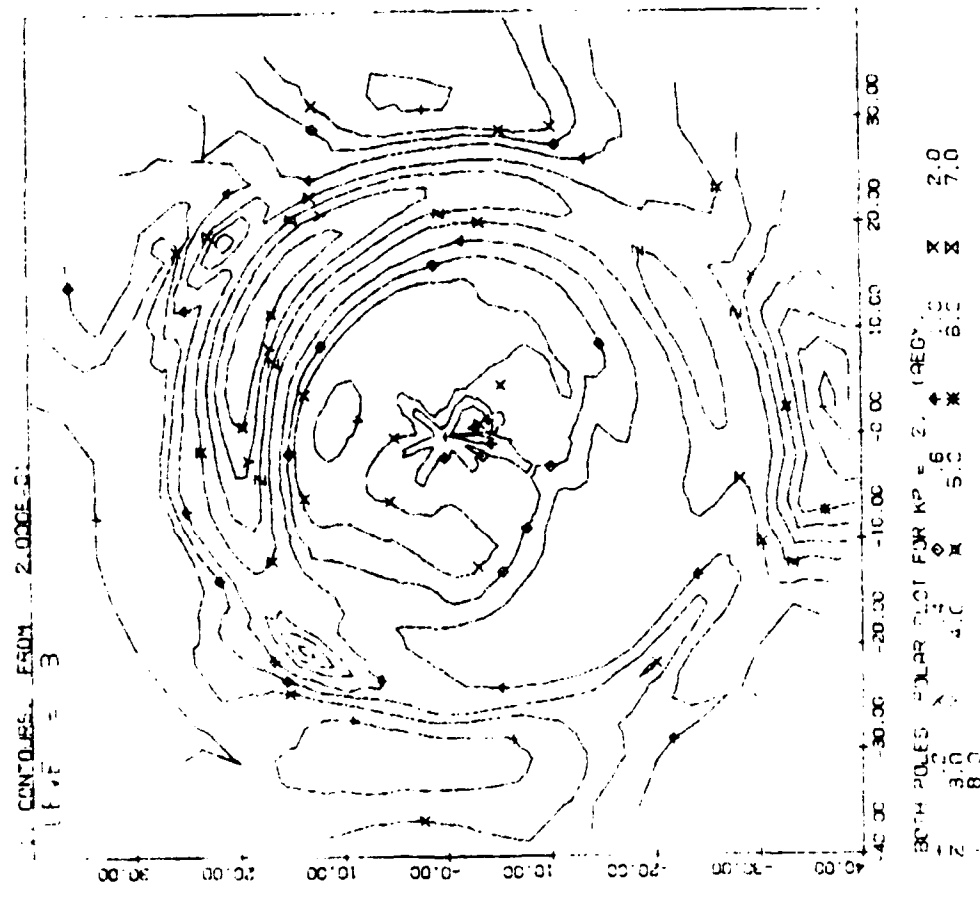


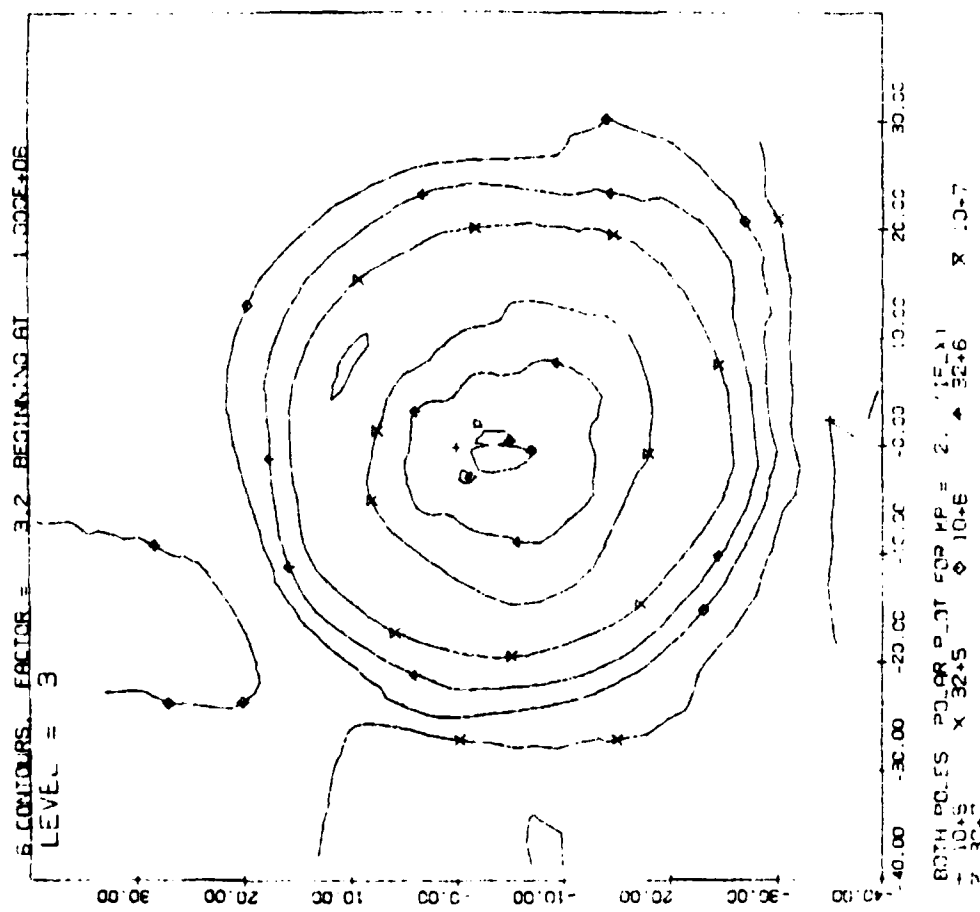


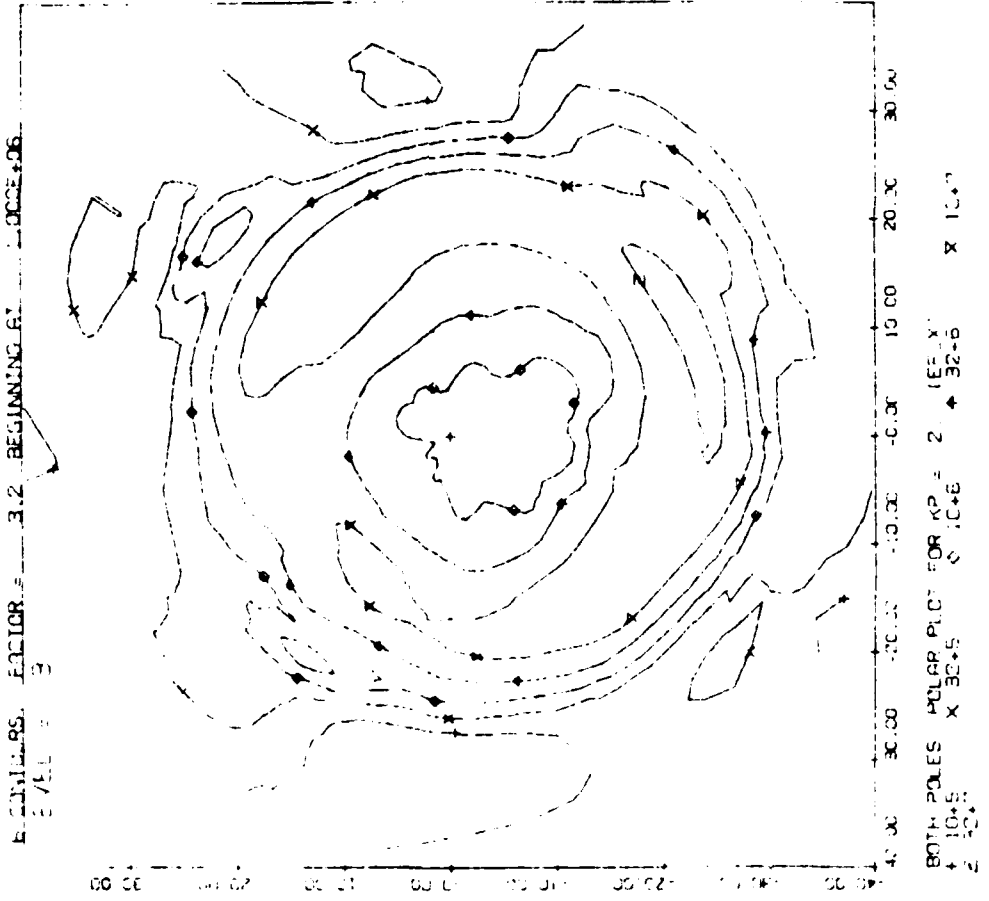


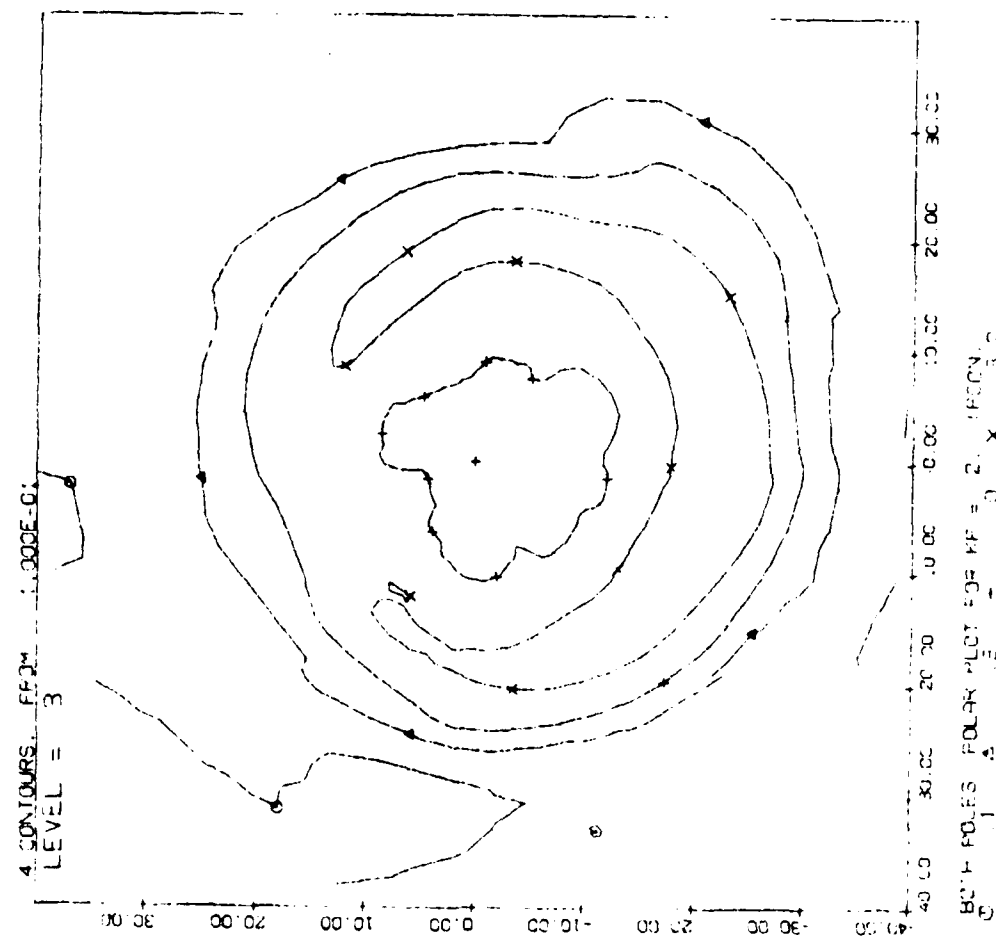


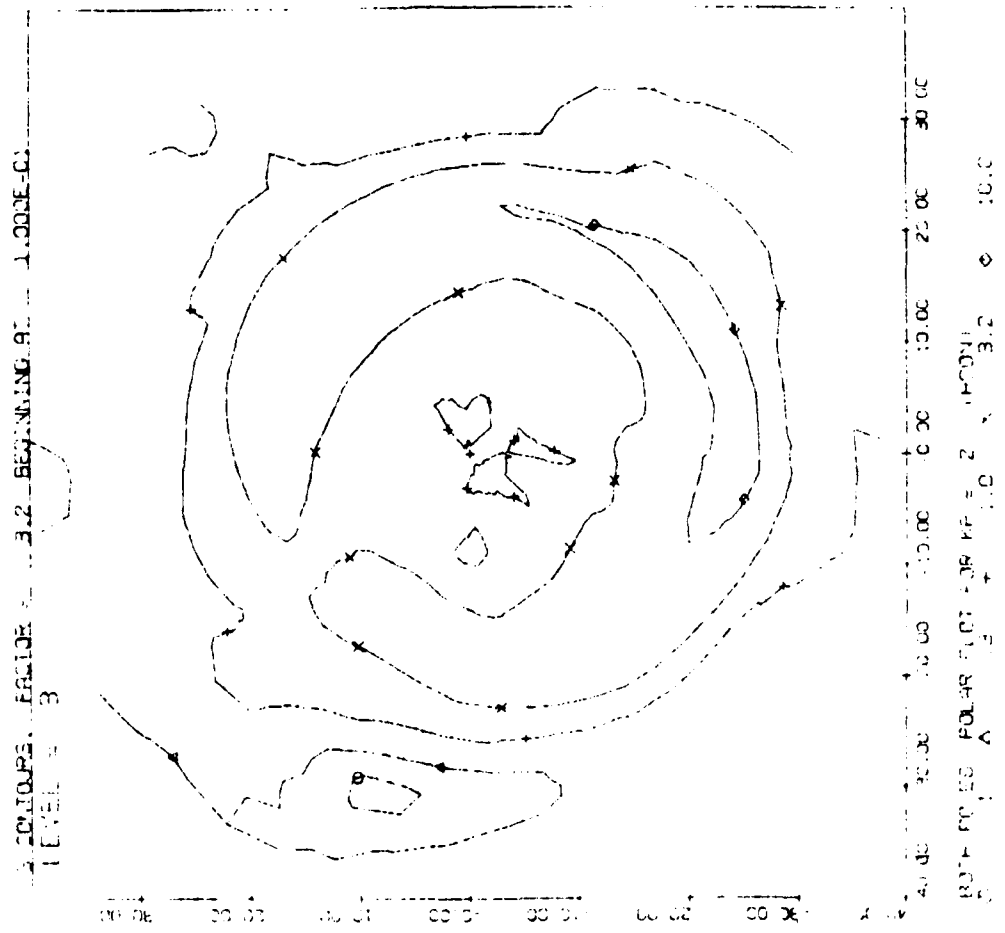


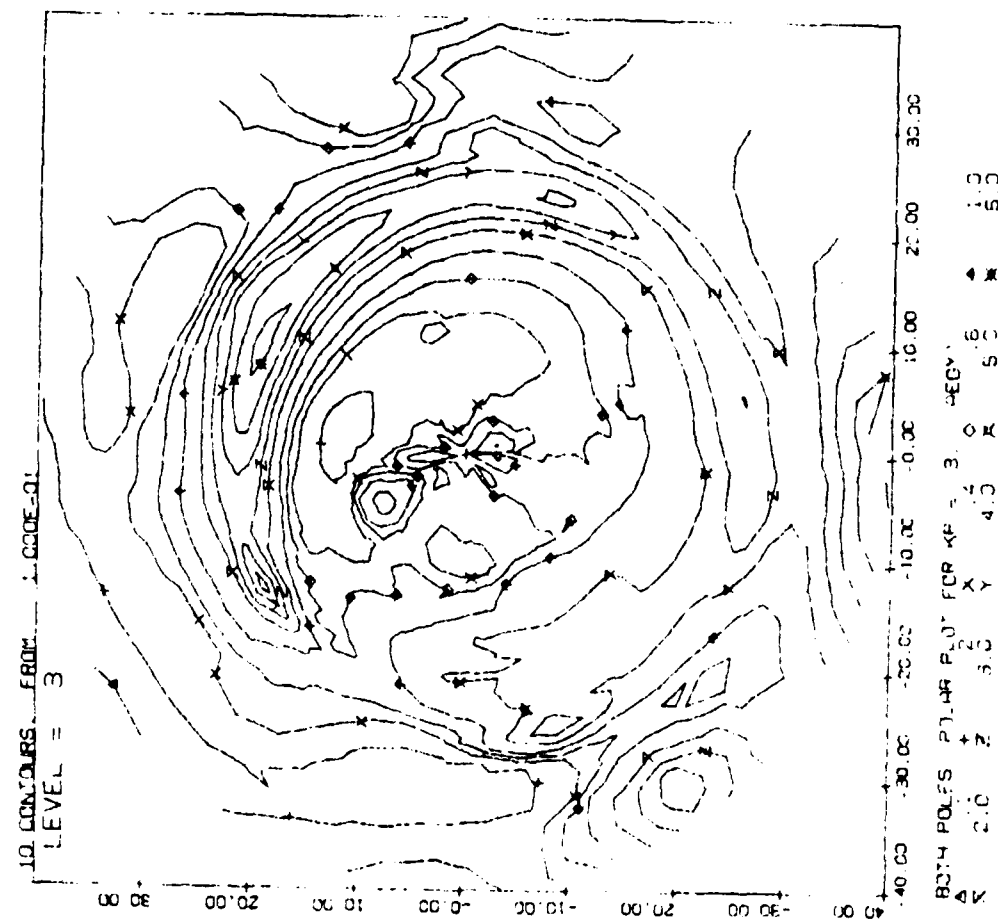


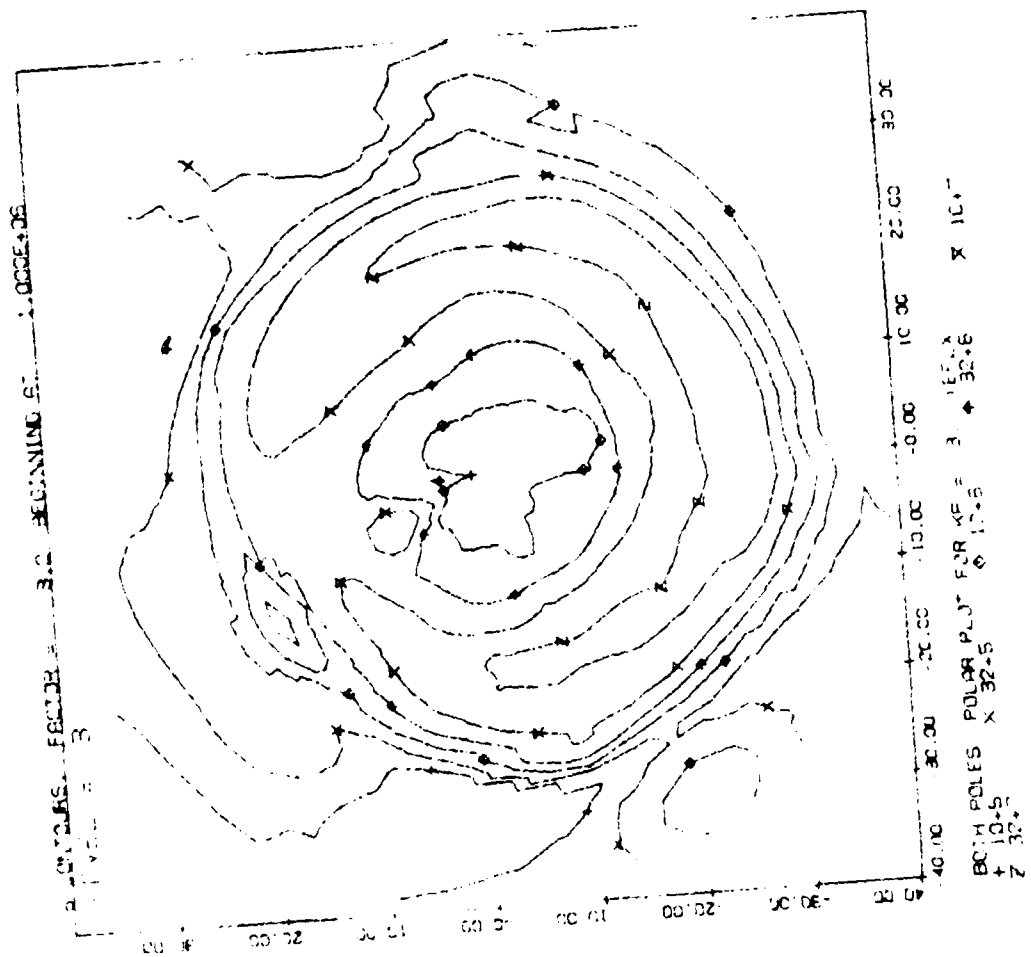


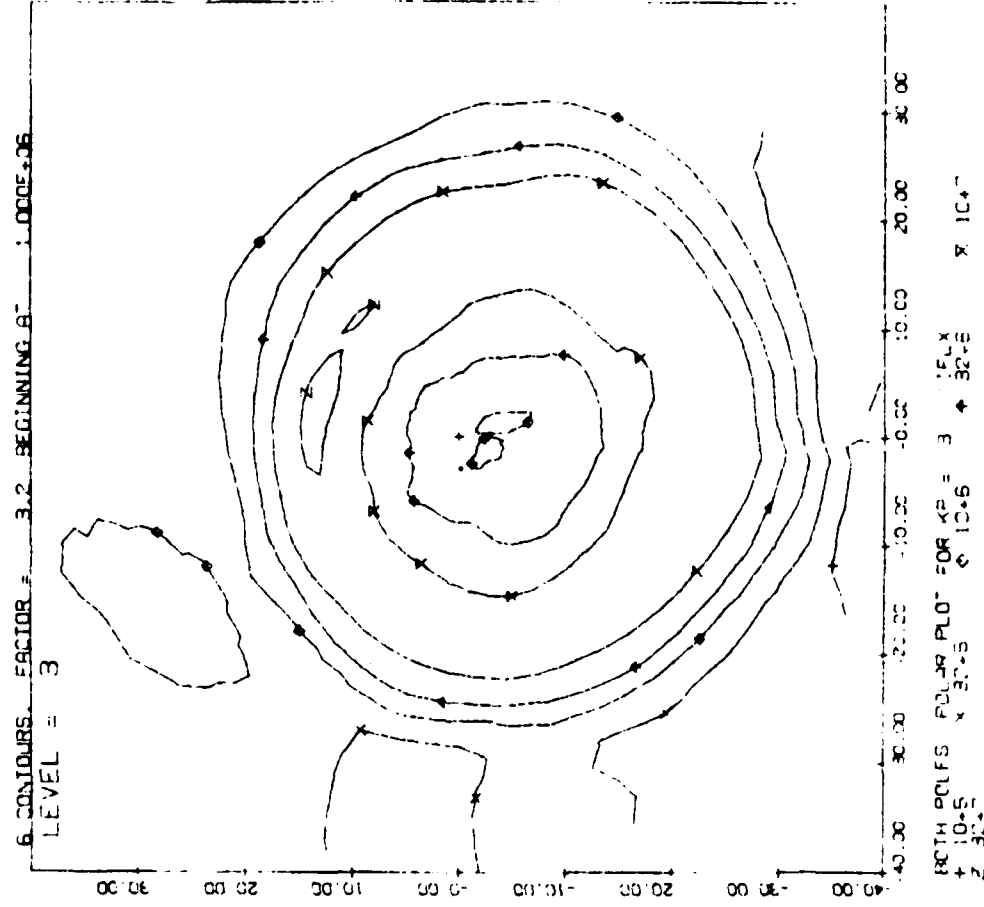


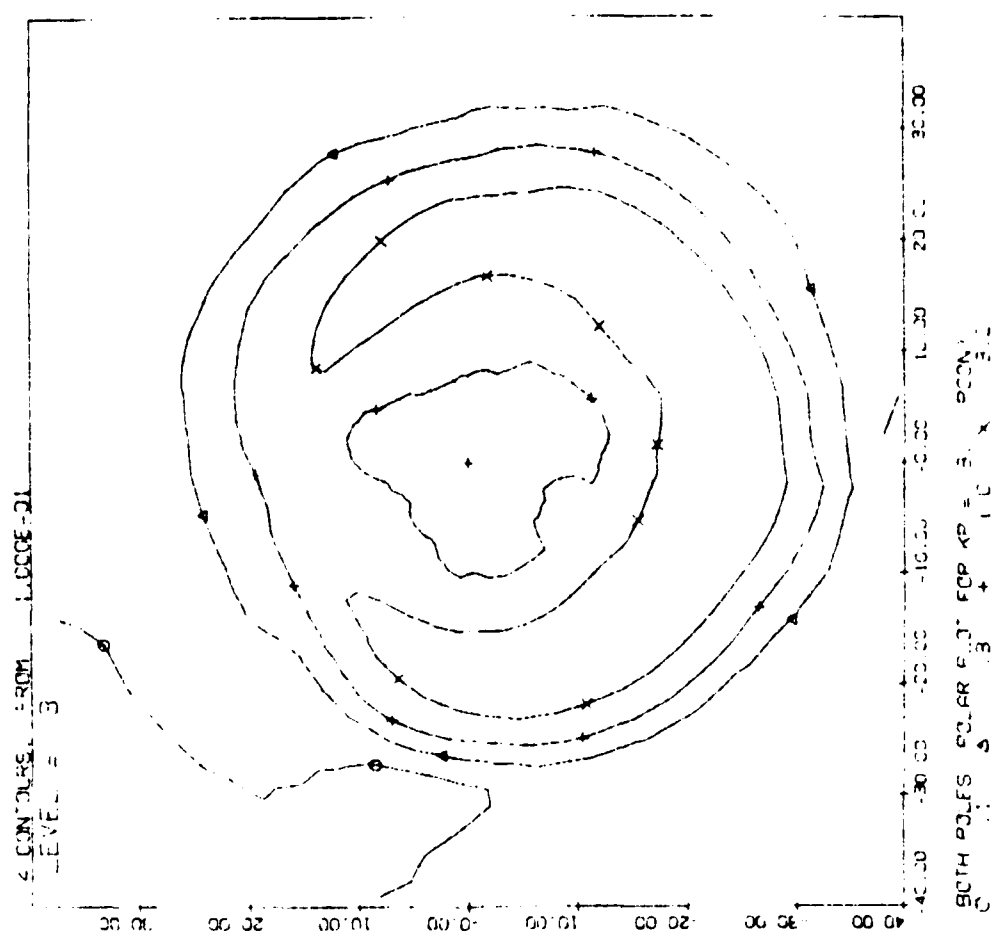


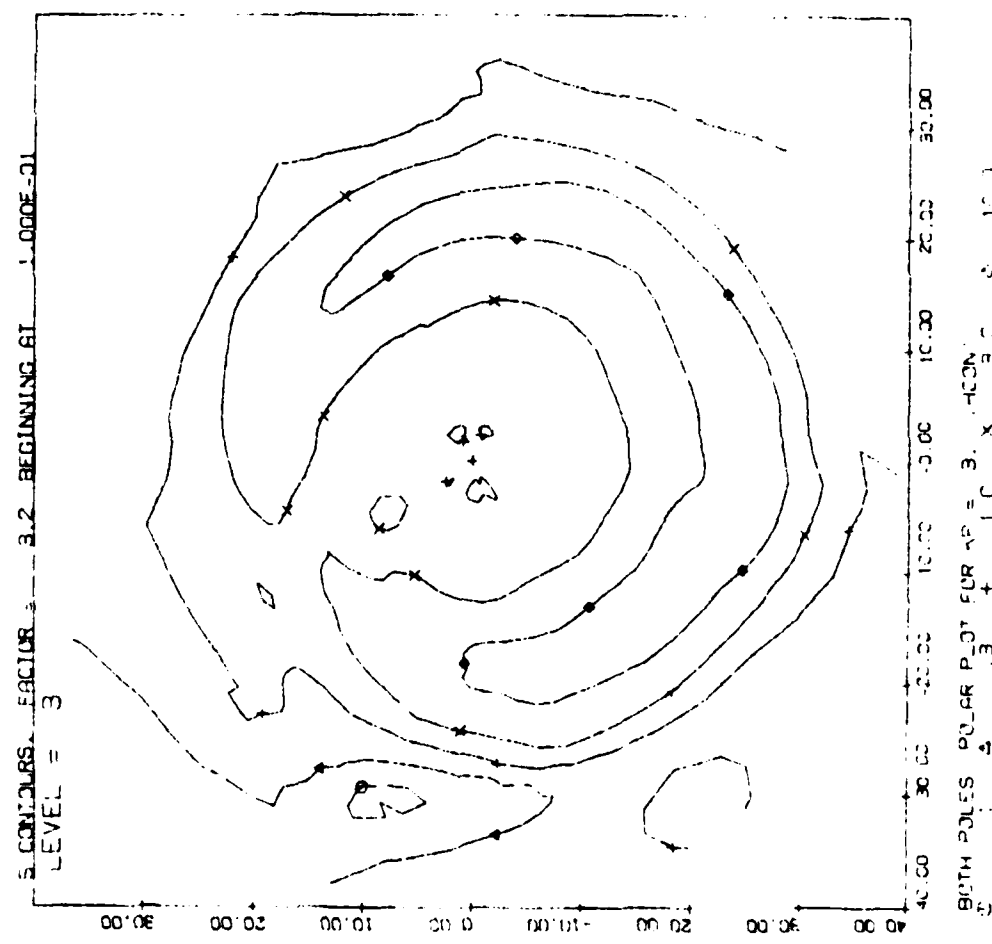


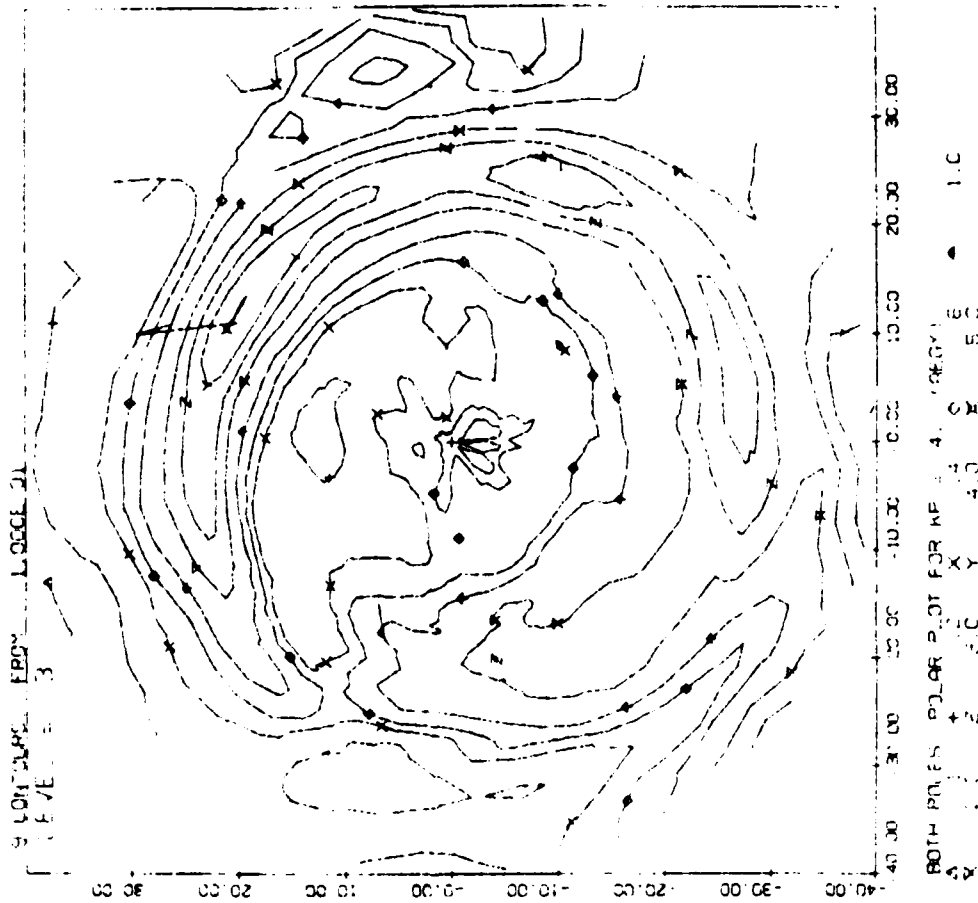


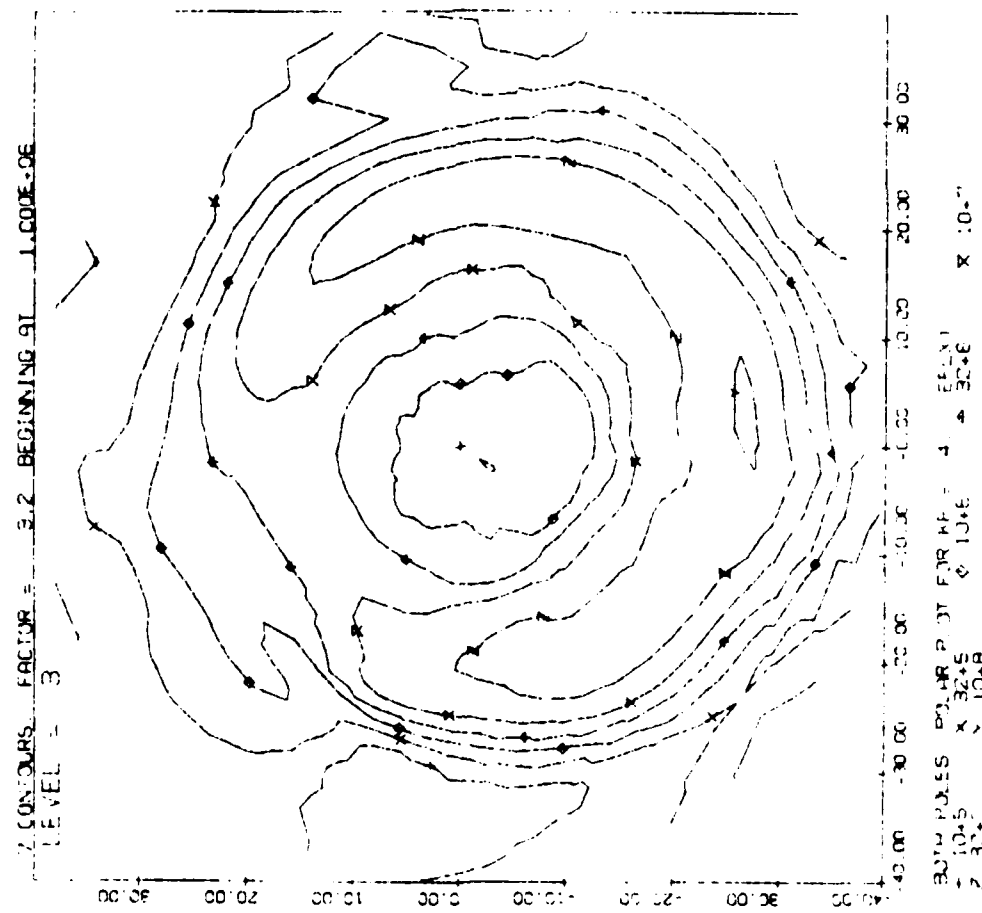


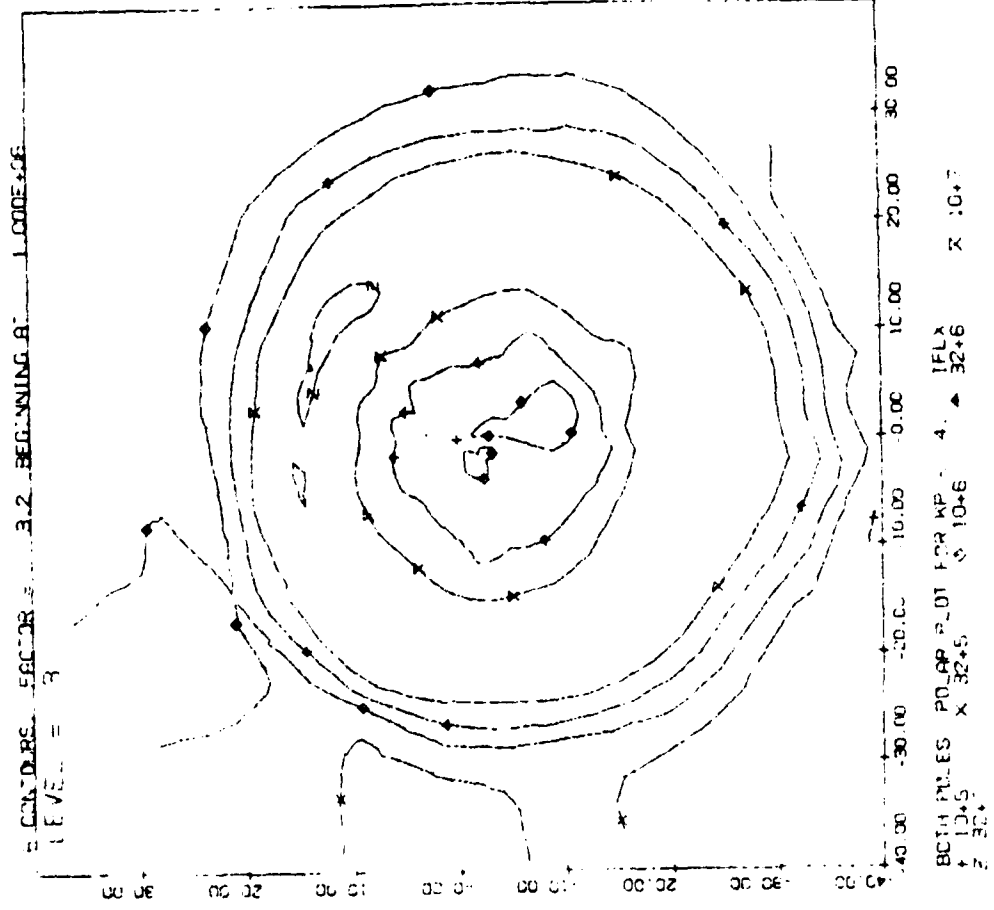


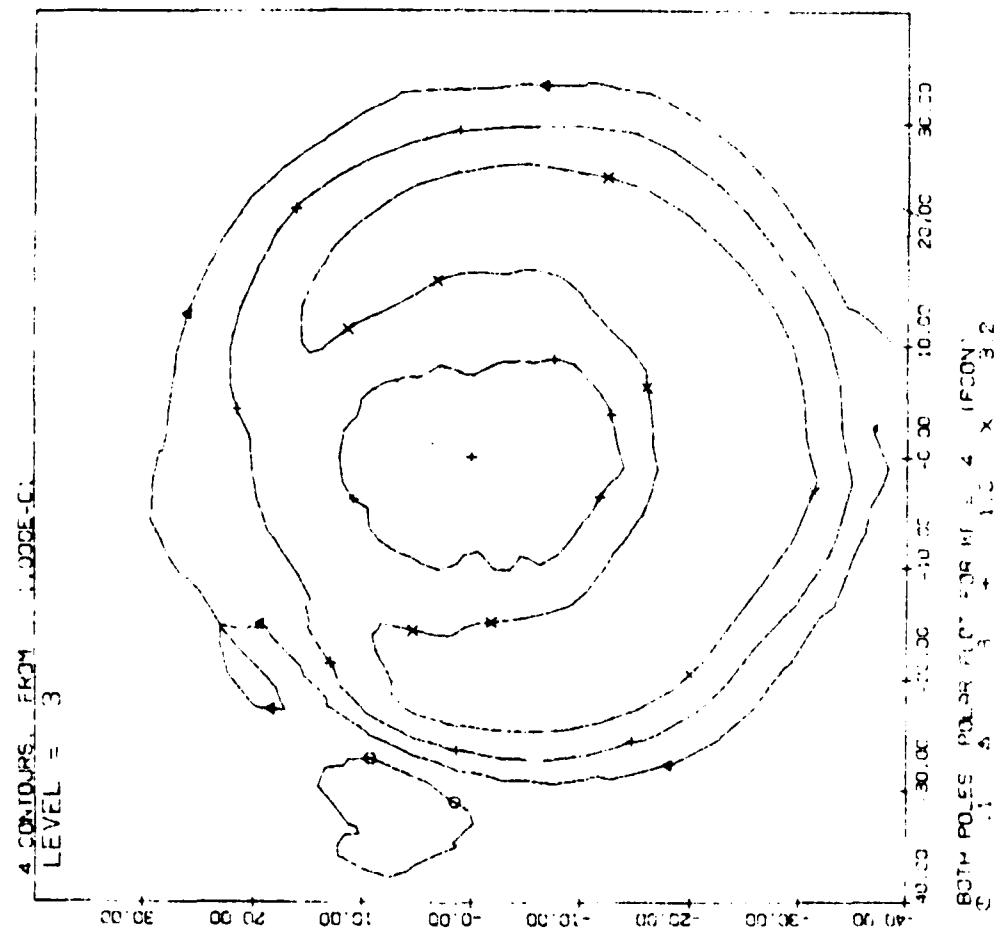


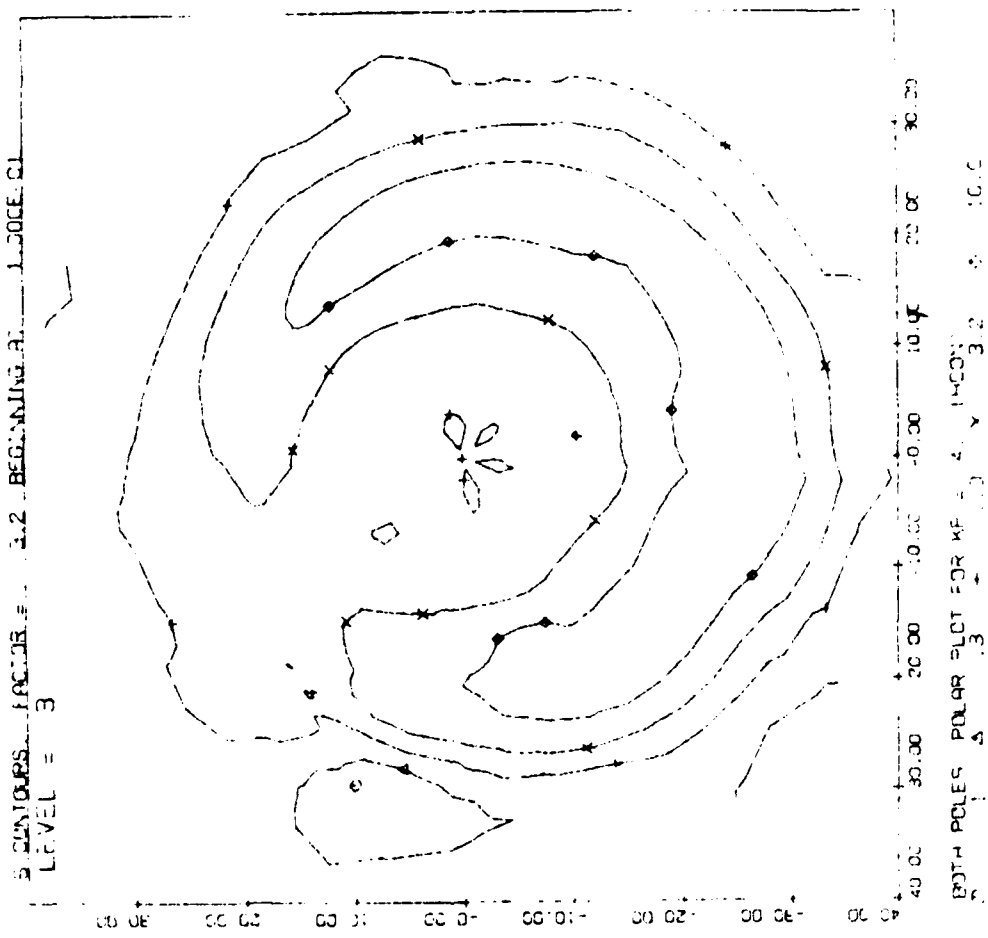


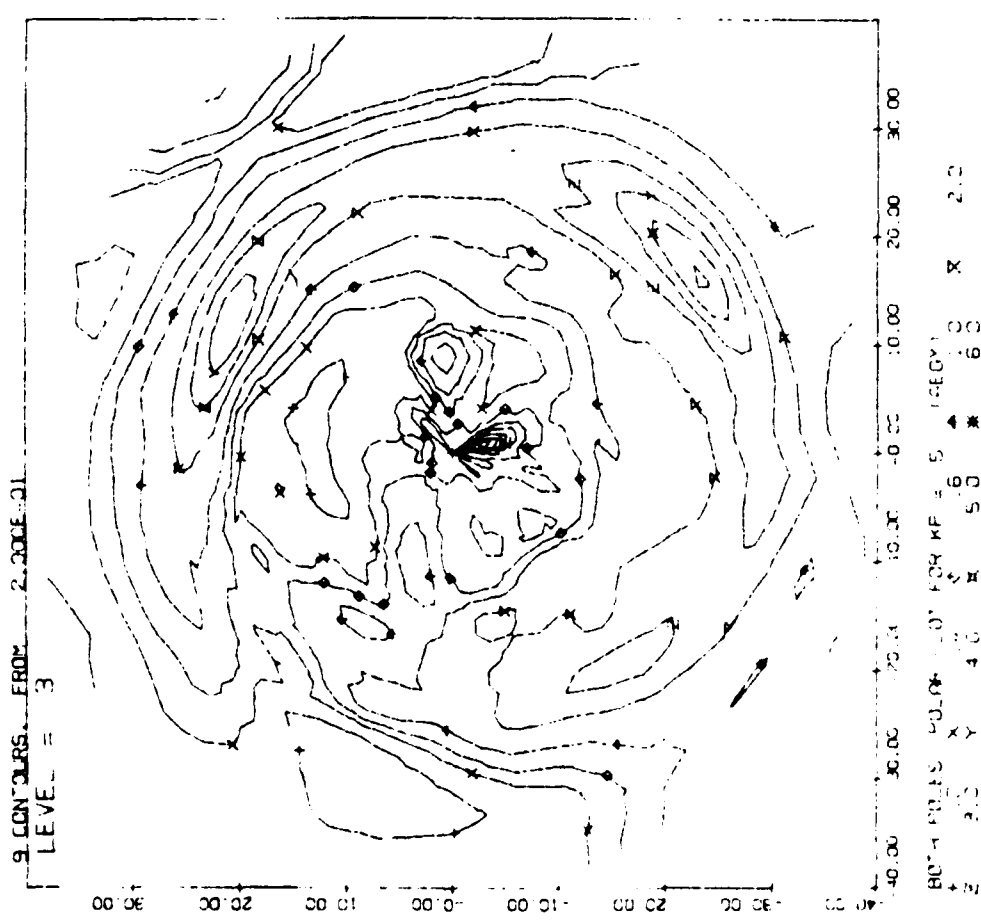


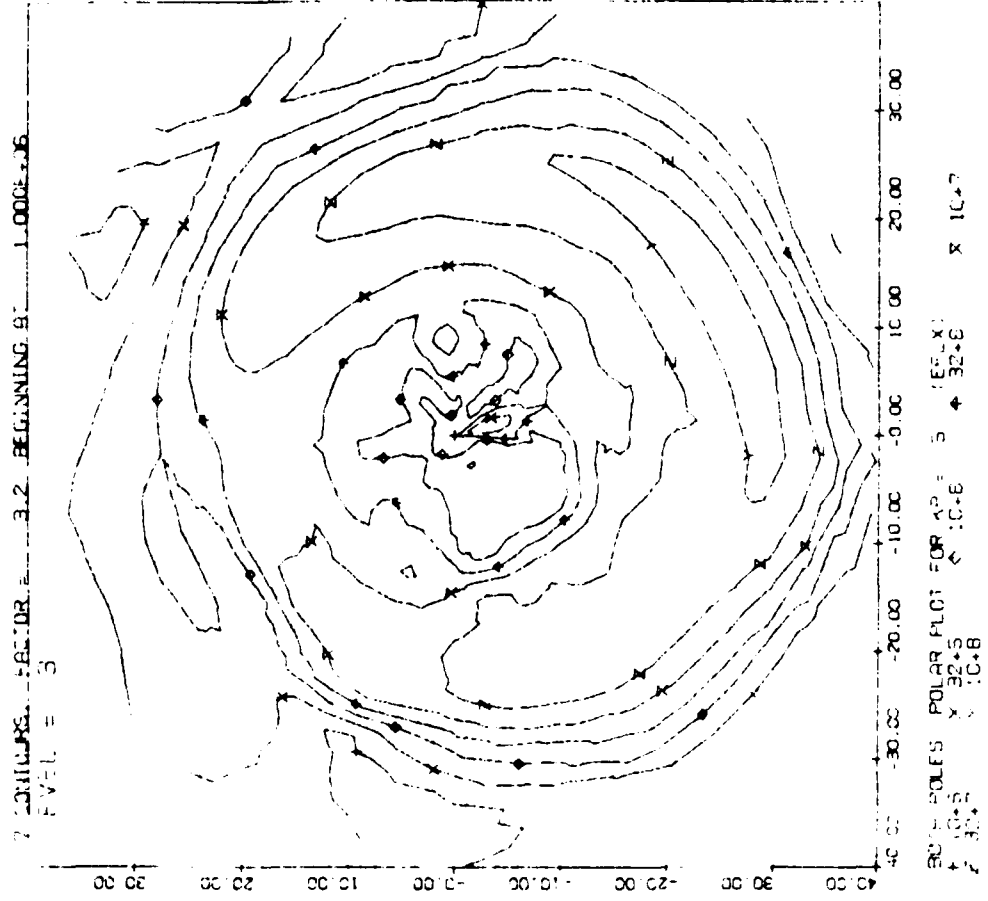


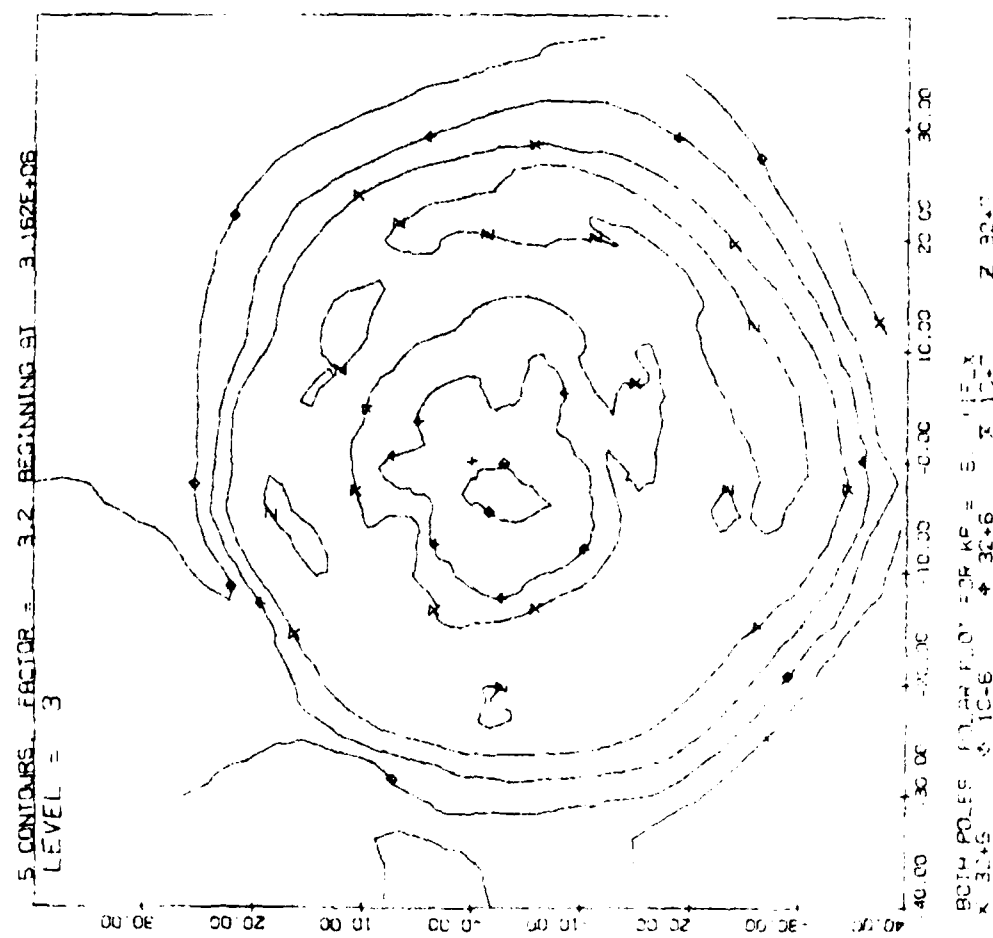


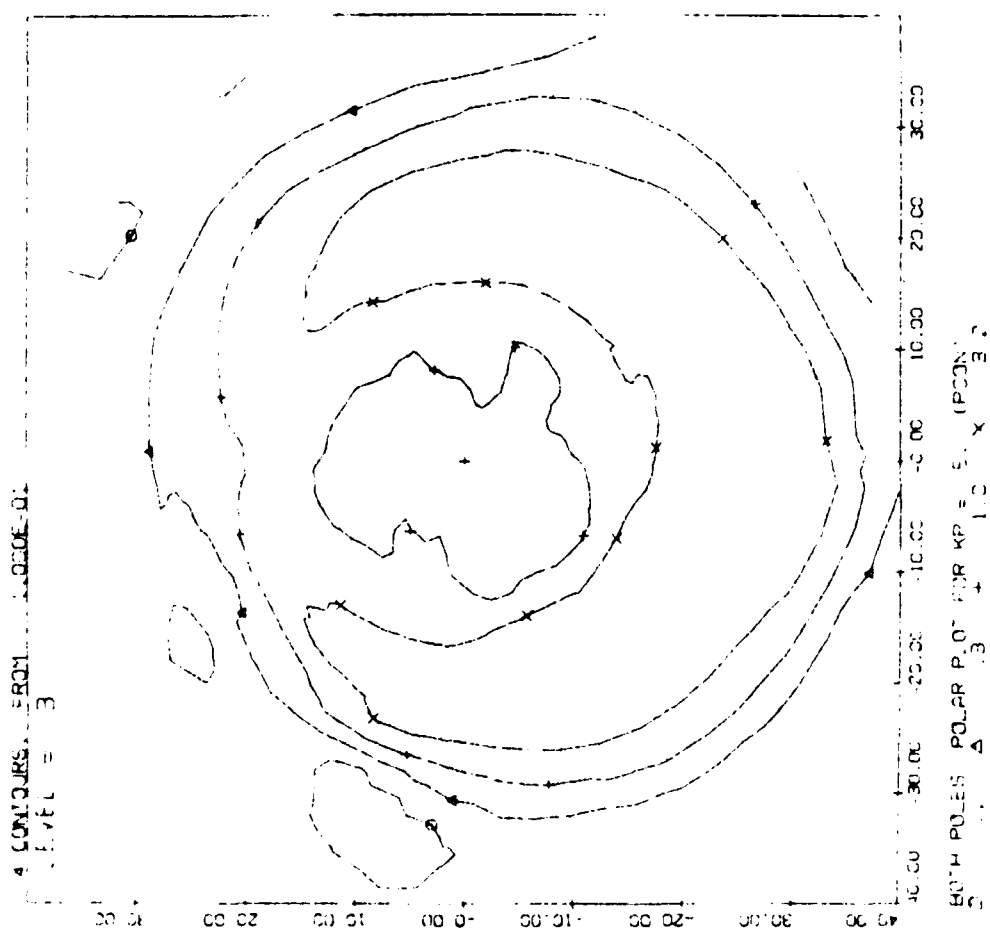


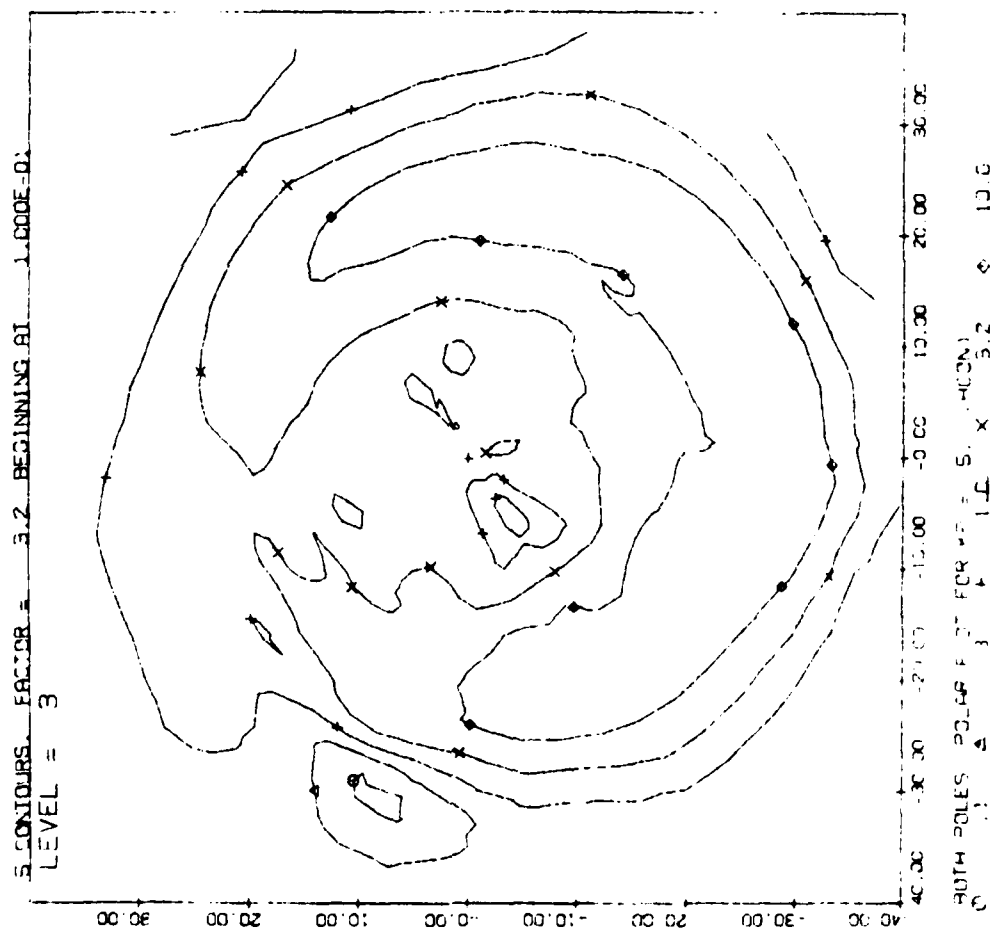


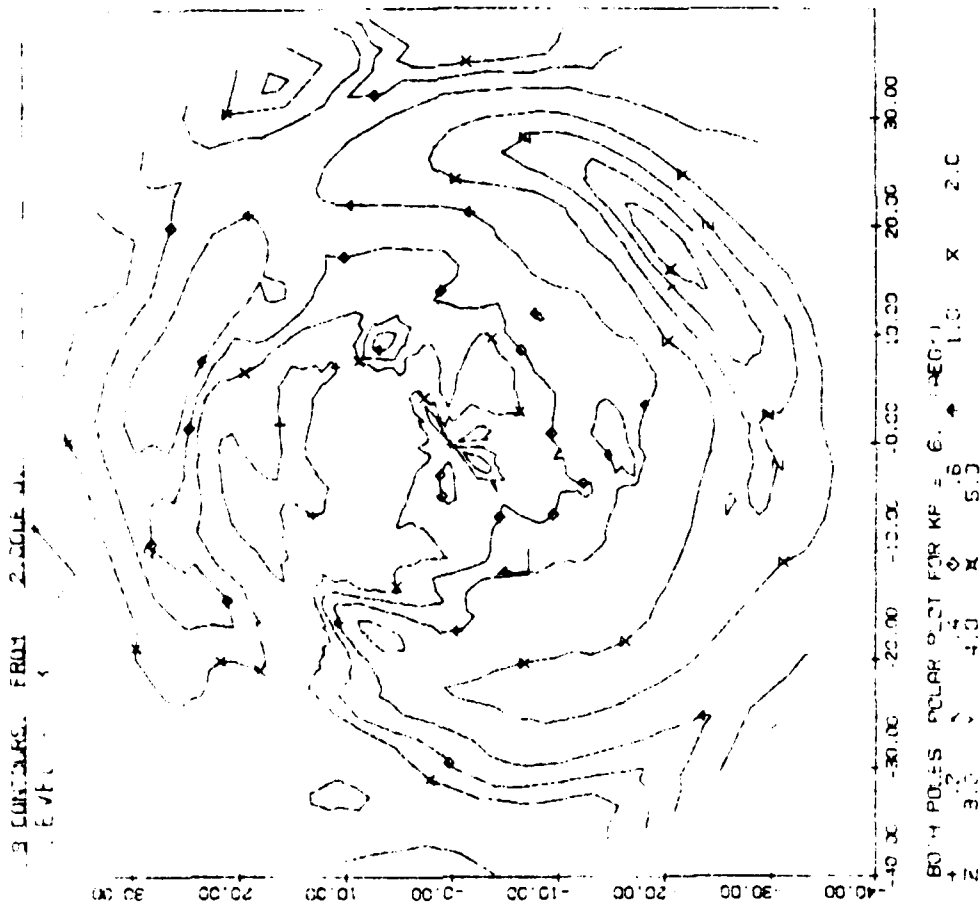


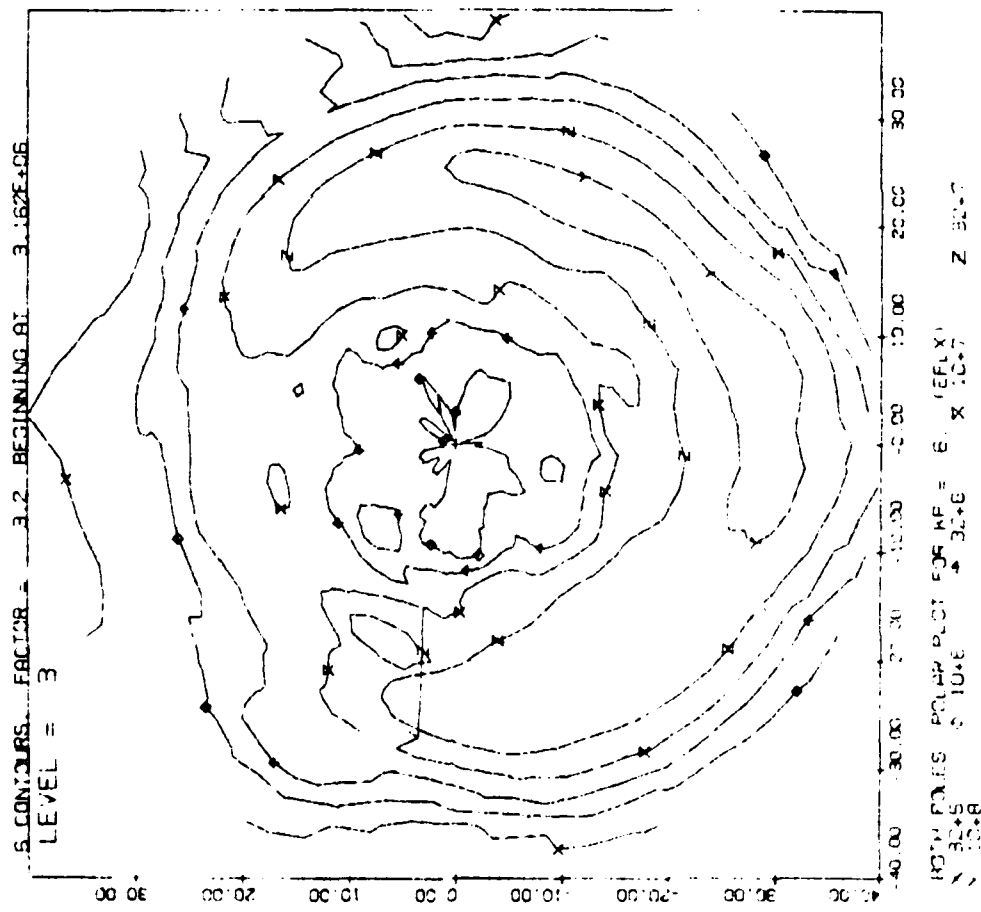


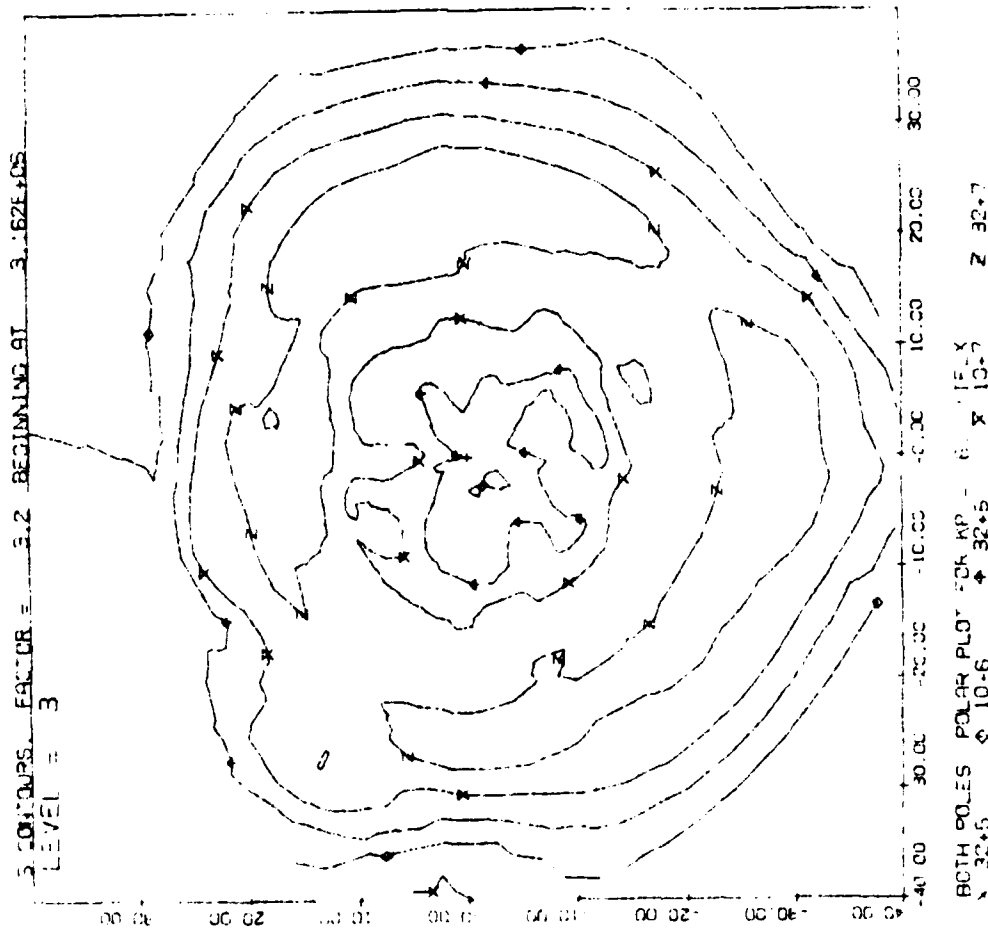




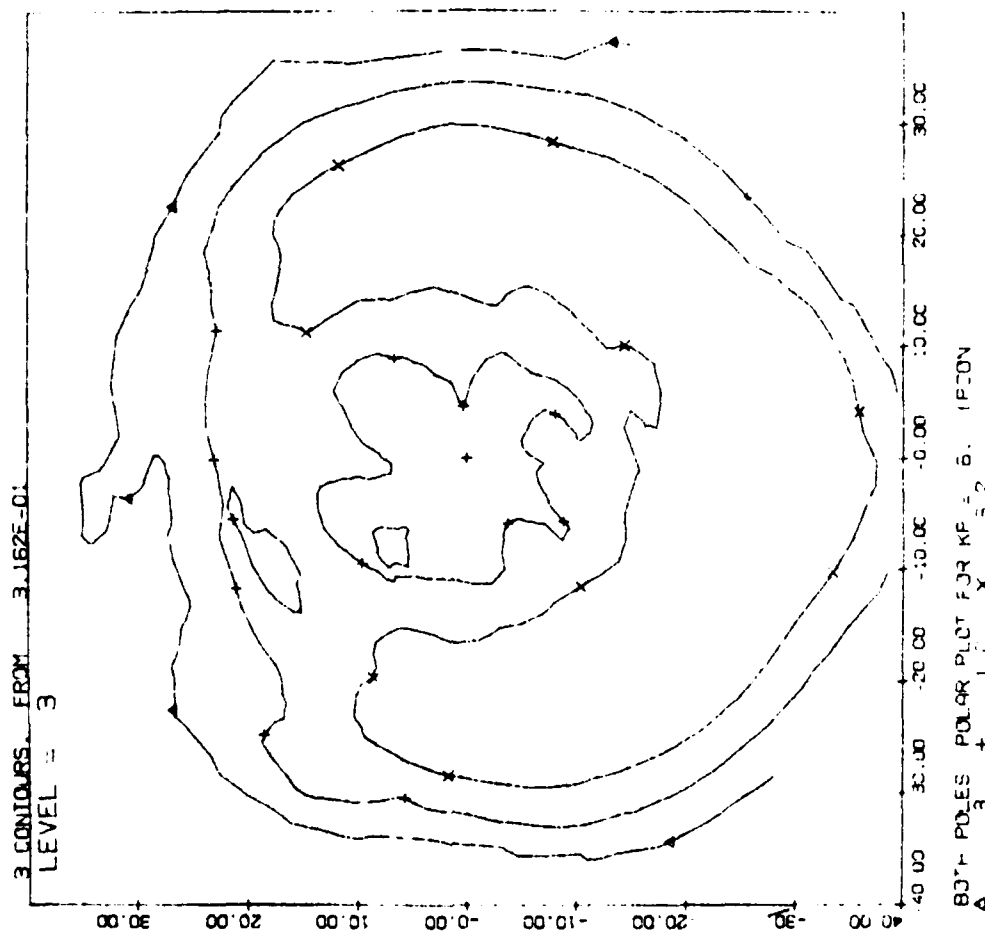


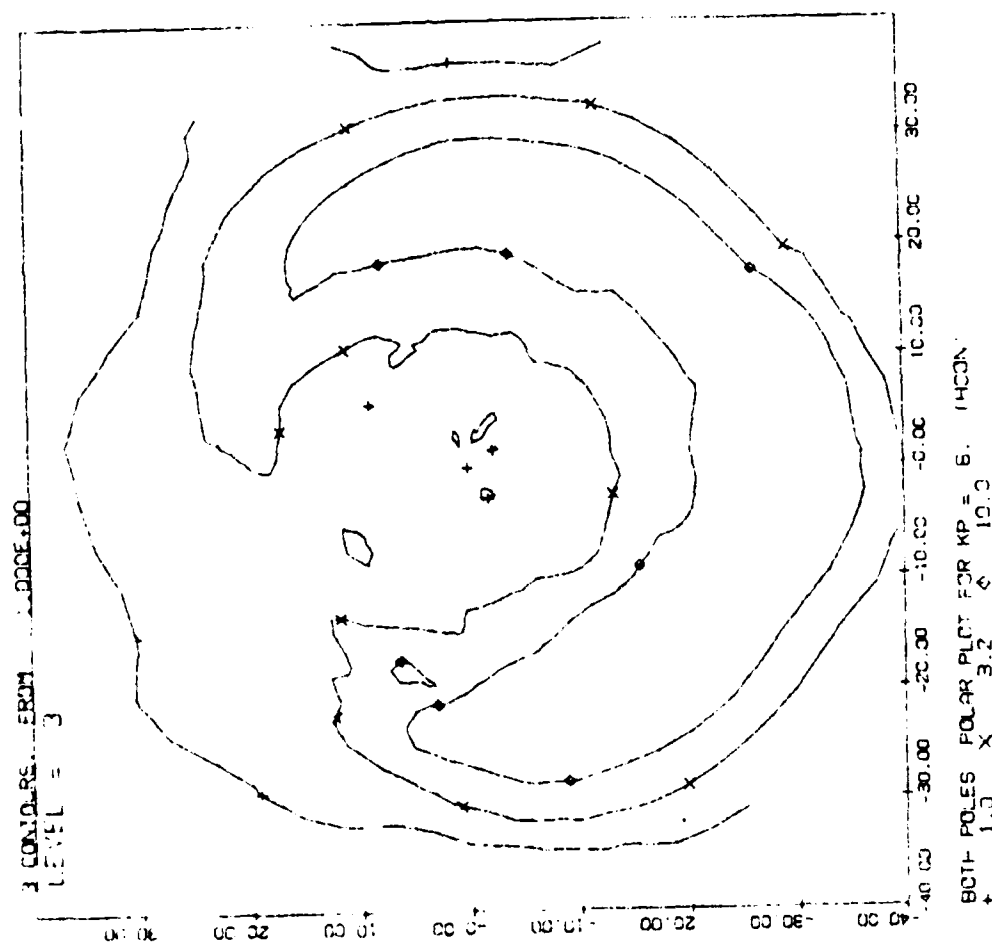






8





END

FILED MED

980

10/10/00
ID: 1010